

Coherent Vector Meson Photo-Production from Deuterium at Intermediate Energies

T.C. Rogers^{a,*} M.M. Sargsian^b M.I. Strikman^a

^a*Department of Physics,
Pennsylvania State University,
University Park, PA 16802, USA*

^b*Department of Physics,
Florida International University,
Miami, FL 33199*

Abstract

We analyze the cross section for vector meson photo-production off a deuteron for photon energies in the intermediate range of energies starting at a few GeVs above the threshold and higher. We reproduce the steps in the derivation of the conventional non-relativistic Glauber expression based on an effective covariant diagrammatic method while making corrections for Fermi motion and intermediate energy kinematic effects. We show that, for intermediate energy vector meson production, the usual Glauber factorization breaks down and we derive corrections to the usual Glauber method to linear order in longitudinal nucleon momentum. The purpose of our analysis is to establish methods for probing interesting physics in the production mechanism for ϕ -mesons and heavier vector mesons. We demonstrate how neglecting the breakdown of Glauber factorization can lead to errors in measurements of basic cross sections extracted from nuclear data.

Key words: Generalized Eikonal Approximation, Vector Meson Production

PACS: 11.80.Fv, 11.80.La

^{*} Corresponding author.

Email addresses: rogers@phys.psu.edu (T.C. Rogers), sargsian@fiu.edu (M.M. Sargsian), strikm@phys.psu.edu (M.I. Strikman).

1 Introduction

Coherent vector meson production from nuclei has proven to be a useful tool for studying the structure of vector mesons. In the very high energy, small angle scattering regime, well above the threshold for vector meson production, the large volume of available experimental data involving proton targets consistently supports the validity of the vector meson dominance (VMD) model for small photon virtualities [1,2]. This, combined with the onset of the eikonal regime in the diffractive region has lead to the development of a successful theoretical framework for the description of vector meson photo-production off nuclei based on the combined VMD model and Glauber theory of hadron-nuclei rescattering [1,3]. The simplicity of the VMD-Glauber framework arises from the fact that at high energies the basic $\gamma N \rightarrow VN$ and $VN \rightarrow NN$ amplitudes vary slowly with the total energy of the γN system relative to the range of important energies in the deuteron wavefunction. This observation leads to the factorizability of the basic $\gamma N \rightarrow VN$ amplitude from the momentum space integral, and yields the conventional Glauber multiple scattering series consisting of non-relativistic form factors and elementary scattering amplitudes.

The VMD-Glauber theory has lead, in particular, to the demonstration that the coherent photo-production of vector mesons off the deuteron at large $-t$ is defined mainly by the rescattering contribution [4]. Since the $VN \rightarrow VN$ amplitude appears in the double scattering term, one may use nuclear photo-production reactions to study the properties of vector mesons [5]. By choosing different t , one can control the relative distance at which rescattering may occur, which allows one to investigate the space-time evolution of hadronic systems produced in electro(photo)- production.

The above program can be extended to the study of coherent vector electro-production at large Q^2 . In this case, coherent vector meson production from the deuteron can be used to study color coherence/transparency phenomena in vector meson electro-production at high Q^2 . The onset of color transparency will reveal itself through the substantial drop in the double scattering contribution with an increase of Q^2 as opposed to the nearly energy independent behavior of the double scattering term for the generalized VMD prediction [5].

In this paper we consider yet another venue of application for vector meson photo-production off nuclear targets by considering photo-production in the intermediate range of energies starting a few GeVs above the threshold. These reactions have great potential for probing several effects such as non-diffractive, OZI violating mechanisms for vector meson production mesons, in-medium modifications of vector mesons, the importance of “non-ideal” $\omega - \phi$ mixing, and other new mechanisms for vector meson production (see

Refs. [6,7,8]).

Finally, it would be interesting to learn whether the ϕ -meson is produced with a small enough transverse size that quark degrees of freedom may become relevant, as in the case of J/ψ -production. Actually, in the case of J/ψ , the cross section of the $J/\psi - N$ interaction $\sigma_{J/\psi - N} \sim 3 \text{ mb}$, [9] estimated based on the A-dependence of J/ψ photo-production at energies $\sim 20 \text{ GeV}$, is much larger than the estimate based on the VDM: $\lesssim 1 \text{ mb}$. This is likely due to the color transparency phenomenon [9]. A natural question is whether a trace of this effect remains in the case of ϕ -production. Jefferson Lab has produced data for J/ψ production that is currently being analyzed.

The interest in intermediate energy reactions makes it necessary to re-evaluate the assumptions of the traditional Glauber series method, and to develop a new theoretical approach. This paper addresses the issues one must face when considering photon energies large enough that the eikonal approximation is an appropriate description of hadronic re-interactions, but not large enough that it is appropriate to neglect vector meson masses in kinematical calculations or any non-trivial s-dependence of the amplitude for photo-production of vector mesons from the nucleon. Furthermore, for small photon energies ($\lesssim 3 \text{ GeV}$) the VMD hypothesis becomes suspect as a description of the $\gamma N \rightarrow VN$ amplitude, so we restrict ourselves to arbitrary photon-nucleon amplitudes. We argue in this paper that there may be a range of photon energies for which the eikonal approximation is valid, but where the usual Glauber theory assumptions of factorization and ultra-relativistic kinematics break down.

Although we retain the eikonal approximation, our approach is distinctly different from the usual Glauber-VMD approach. In particular, one of the basic assumptions used in the Glauber approach is that the basic $\gamma N \rightarrow VN$ and $VN \rightarrow VN$ cross sections are slowly varying functions of center of mass energy and that the small Fermi momentum of the nucleons can be neglected in the evaluation of the total energy of the γN and VN systems. These assumptions result in the usual factorizability already discussed above. At intermediate energies, however, the photon energy is comparable to the vector meson mass, and the basic amplitude may gain non-trivial energy dependence due to the fact that Regge theory may be inadequate at intermediate photon energies. The usual smooth, slow rise in the total $\gamma N \rightarrow VN$ cross section characteristic of high energy diffractive scattering may be absent at intermediate energies. Fermi motion effects thereby destroy the factorizability of nuclear scattering into basic amplitudes and form factors. Also, the longitudinal momentum transferred (proportional to M_V^2/E_γ) plays an important role as compared to reactions in the diffractive regime and further calls into question the factorization assumption. Earlier work (e.g. [1]) has considered the effect of longitudinal momentum transfers, but the breakdown of factorization has been ignored.

To summarize, the kinematic situations under consideration in this paper are such that the produced vector mesons are energetic enough for the eikonal approximation to be valid. However the energy dependence of the $\gamma N \rightarrow VN$ amplitude due to the break down of very high energy assumptions will require that we account for Fermi motion effects which, in turn, will require that we account for non-factorization effects. In the derivation of the total $\gamma D \rightarrow VD$ amplitude we will use the generalized eikonal approximation [10,11] which is the approximation, valid at appropriately high energies, that allows us to derive the scattering amplitudes starting with corresponding effective Feynman diagrams while neglecting multiple scattering from the same nucleon. (It is referred to as “generalized” in this case because it is used for inelastic reactions.)

By maintaining the result in terms of momentum space integrals, both transferred longitudinal momentum and Fermi motion effects may be explicitly taken into account consistently. In our derivations, we keep only the corrections to the basic amplitudes that are of linear order in longitudinal exchanged momentum or nucleon momentum (neglecting order \mathbf{k}_N^2/m_N^2 corrections, where \mathbf{k}_N is the bound state nucleon momentum). This allows us to relate $D \rightarrow NN$ transition vertex to the nonrelativistic wave function of the deuteron. Since dynamical, model-dependent corrections related to the N-N interaction are expected to be of quadratic or higher order in nucleon momentum, then linear order corrections arising from intermediate energy kinematics should be taken into account *before* any specific theory of the basic bound state amplitude that deviates from the nearly flat behavior of Regge theory is used in the typical Glauber theory.

We also note that the basic amplitude for $\gamma N \rightarrow VN$ scattering is obtained directly from experimental data with a nucleon target. The secondary scattering amplitude is usually determined from the VMD hypothesis at high energies, but the use of VMD is suspect at energies of only a few GeVs. A formalism should be maintained that allows the $\gamma N \rightarrow VN$ and the $VN \rightarrow VN$ amplitudes to be independently modeled. Fitting data to our modified form of the Glauber theory by using the $VN \rightarrow VN$ amplitude as a parameter allows one to infer a value for the $VN \rightarrow VN$ cross section.

The paper is organized as follows: In Sec. 2 we derive scattering amplitudes for the $\gamma D \rightarrow VD$ reaction based on the generalized eikonal approximation. In Sec. 3 we discuss the steps needed to take into account linear order corrections in nucleon momentum. In Sec. 4 we perform a sample calculation where we compare our results at intermediate energy kinematics with the prediction of conventional VMD-Glauber theory. We identify the effects which are responsible for the divergence of the our prediction from the Glauber theory. We demonstrate that effects calculated in this paper, if unaccounted for, can yield a misinterpretation of the VN scattering cross section if it is extracted from

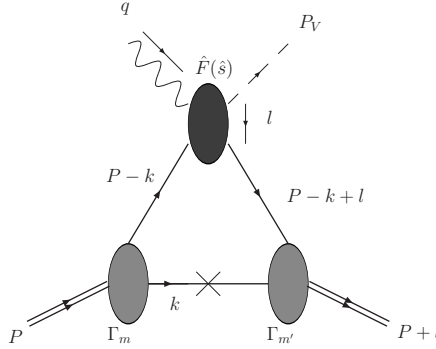


Fig. 1. The impulse diagram for photo-production. The cross on the spectator nucleon line indicates that the spectator nucleon will be taken on shell in the non-relativistic approximation. (For all Feynman graphs we use Jaxodraw [12].)

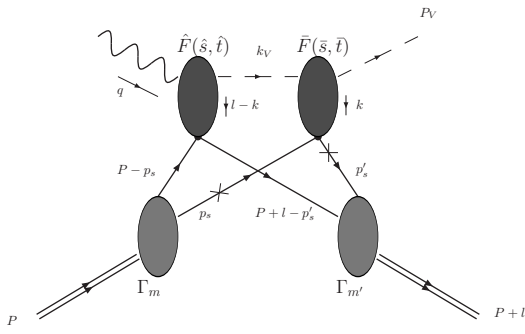


Fig. 2. The double scattering diagram for photo-production.

the data using the usual Glauber approximation. In Sec. 6 we summarize our results. In Appendix A we describe the model of the basic amplitude that we used for our sample calculation, and in Appendix B we give an overview of the usual treatment of deuteron spin in Glauber theory.

2 Formulae for the Amplitudes

2.1 Reaction and Kinematics

We study the coherent photo-production of vector mesons off the deuteron in the reaction:

$$\gamma + D \rightarrow V + D', \quad (1)$$

where $P \equiv (M_D, 0)$ and $P' \equiv (E_D, \mathbf{P}')$ define the initial and final four momenta of the deuteron. We use natural units ($c = \hbar = 1$). The relevant effective Feynman graphs in the eikonal approximation are shown in Figs. 1 and 2. $q \equiv (E_\gamma, \mathbf{q})$ and $P_V \equiv (E_V, \mathbf{P}_V)$ define the 4-momenta of the initial photon and the final state meson respectively. The three-momentum transferred is

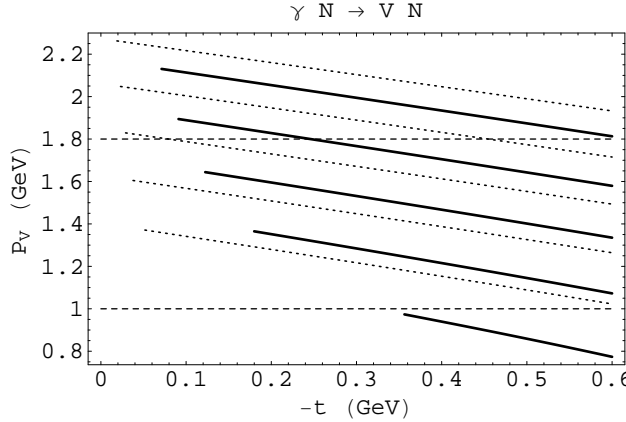


Fig. 3. Vector meson 3-momentum produced by a photon scattering from a nucleon target as a function of $-t$ for a given set of fixed E_γ . The solid lines correspond to ϕ -meson production, whereas the dotted lines correspond to ρ^0 -meson production. The incident photon energies in each case, going from the bottom curve to the top curve are 1.6, 1.8, 2.0, 2.2, 2.4 GeV. The dashed lines at $P_V = 1$ GeV and $P_V = 1.8$ GeV may be viewed as separating the intermediate range of energies where our approach (as applied to ϕ -meson production) is justified from the range of energies that are too low to be considered here. Above the line at $P_V = 1.8$ GeV, the GEA is a very good approximation, and it is this part of the graph that corresponds to the region of kinematics we are interested in. Below $P_V = 1.0$, neither the usual Glauber Approach, nor our approach should be applied.

defined as $\mathbf{l} = \mathbf{q} - \mathbf{P}_V$. In our calculations we concentrate intermediate energy kinematics.

We will assume that we are discussing the region of kinematics where we may apply the Generalize Eikonal Approach (GEA) [11] which allows us to ignore multiple scattering by the same nucleon. (It is “general” because it applies in this case to inelastic scattering.) The GEA is the “straight line” approximation; the incident particle follows a nearly straight line path through the nucleus. Clearly this must occur at high enough energies that higher partial waves than just the s -wave contribute. In order to establish the appropriate kinematical regime for our approach, we have plotted in Fig. 3 the lab frame 3-momentum of the final state vector meson as a function of $-t$ for a set of incident photon energies for the case of ρ^0 and ϕ -meson production from a nucleon. We see that, as the photon energy increases, the eikonal regime is quickly approached at small $-t$. This demonstrates that it is possible, even at rather low energies, to apply the GEA to the reaction of Eq.(1) as long as the 3-momentum of the final state vector meson is chosen appropriately. The experience of the application of the Glauber model to the description of proton-nucleus scattering [13] indicates that the eikonal approximation works roughly for $p_N/m_N \gtrsim 1$ GeV and it works extremely well for $E \gtrsim 2m_N$. Since $m_\phi \sim m_N$ we expect the onset of the GEA for a similar range of momenta for ϕ -meson production. We continue to use the criterion that $E \gtrsim 2M_V$, and find

that the value of vector meson 3-momentum where the GEA may certainly be applied is $P_V \gtrsim 1.8$ GeV for ϕ -meson production. The values of 3-momentum, 1 GeV and 1.8 GeV have been indicated by horizontal dashed lines in Fig. 3. These dashed lines in Fig. 3 may be viewed as separating kinematic configurations where our approach may be applied to ϕ -meson production from kinematic regions where both our approach and the Glauber approach should be abandoned entirely with regards to ϕ -meson production. Below $P_V \approx 1$ GeV, both our approach and the usual Glauber approach should be abandoned. Between 1 GeV and 1.8 GeV, the GEA may become a rough approximation, but above 1.8 GeV, our approach using the GEA is a very good approximation. For example, in the case of ϕ -meson production at $E_\gamma = 1.6$ GeV, the solid curve in Fig. 3 is below the dashed line at 3-momentum $P_V = 1.0$ GeV for the entire allowed range of t . This lies outside the regime of applicability of our approach, and we make no claims about this region of kinematics. On the other hand, for $E_\gamma \gtrsim 2.4$ GeV, the 3-momentum of the produced ϕ -meson lies well above 1.8 GeV for the whole range of t so that the GEA is expected to be valid. Our main interest in this paper is the production of the ϕ -meson at around 3 GeV, so the application of the GEA is quite safe. We will find that another problem arises at $t \approx t_{min}$, and this will be discussed in Sec. 4, but the above argument remains the same as long as $-t$ is more than a few tens of MeVs larger than $-t_{min}$. We further assume that the non-relativistic model of the $N - N$ interaction can be represented by a $D \rightarrow NN$ vertex. In the case of the deuteron, there are only two relevant diagrams: the single scattering diagram (Born term) of Fig. 1 and the double scattering diagram of Fig. 2.

As illustrated in Fig. 2, the double scattering term has two distinct interaction vertices. The vector meson is produced at the first vertex and re-scatters from the second. In this it is reminiscent of nucleon knock-out reactions, in which a fast nucleon is knocked out at the first vertex and then re-scatters from spectator nucleons. The fact that, as Fig. 3 demonstrates, the intermediate vector meson may carry high momentum, even relatively near to threshold, is essential since it allows us to use the GEA approach to calculate the scattering amplitudes corresponding to the diagrams of Fig 1 and Fig. 2.

2.2 The Born Amplitude

We start with the calculation of the amplitude corresponding to the Born term of Fig. 1. $F_{m,m'}^0(s, t)$ will denote the $\gamma D \rightarrow VD$ scattering amplitude for the Born term in which only one of the nucleons takes part in the interaction, whereas $\hat{F}(\hat{s}, t)$ will denote the basic $\gamma N \rightarrow VN$ scattering amplitude. A hat on a variable indicates that it is associated with the $\gamma N \rightarrow VN$ subprocess rather than the process of Eq. (1). The superscript, 0, is meant to distinguish this term from the double scattering term. The initial and final polarizations

of the deuteron are denoted by m and m' respectively. Because of the nearness to threshold, the $\hat{F}(\hat{s}, t)$ amplitude is not necessarily diffractive and we do not assume the validity of the VMD hypothesis. We neglect the spin-flip component of the basic amplitude (i.e. \hat{F} and \bar{F} are approximately diagonal in nucleon spin.) The $D \rightarrow NN$ vertex is denoted by Γ_m . For simplicity, information on the spin structure is absorbed into Γ_m . All variables correspond to the labels in the Feynman diagram of Fig. 1 for the single scattering (Born) term. The free nucleon mass is denoted by m_N .

By applying effective Feynman rules to the graph in Fig. 1 we obtain the manifestly covariant scattering amplitude,

$$\begin{aligned} F_{m,m'}^0(s, t) = & \\ & - \int \frac{d^4 \mathbf{k}}{i(2\pi)^4} \frac{\Gamma_{m'}^\dagger(P - k + l) \hat{F}(\hat{s}, t) \Gamma_m(P - k)}{[(P - k + l)^2 - m_N^2 + i\epsilon] [(P - k)^2 - m_N^2 + i\epsilon] [k^2 - m_N^2 + i\epsilon]} \\ & + (p \leftrightarrow n). \end{aligned} \quad (2)$$

$(p \leftrightarrow n)$ refers to the term in which the neutron and proton are inverted. In the remainder of this text, Mandelstam variables that appear within an integral are understood to be functions of internal nucleon 4-momentum and the incident photon 4-momentum.

We proceed with the derivation by estimating the loop integral in Eq.(2) up to terms of order $\frac{\mathbf{k}^2}{m_N^2}$. This approximation allows us to evaluate the integral in Eq.(2) by keeping only the pole contribution which yields a positive energy for the spectator nucleon. We find,

$$\begin{aligned} F_{m,m'}^0(s, t) = & \int \frac{d^3 \mathbf{k}}{(2\pi)^3} \frac{\Gamma_{m'}^\dagger(P - k + l) \hat{F}(\hat{s}, t) \Gamma_m(P - k)}{2k_0 [(P - k + l)^2 - m_N^2 + i\epsilon] [(P - k)^2 - m_N^2 + i\epsilon]} \\ & + (n \leftrightarrow p). \end{aligned} \quad (3)$$

(Note that $k_0 = m_N$ up to correction terms of order \mathbf{k}^2/m_N^2 .) We now make use of the correspondence between the non-relativistic wave function and the vertex function,

$$\tilde{\Psi}_m(\mathbf{k}_{rel}) \equiv \frac{-\Gamma_m(P - k)}{2\sqrt{k_0(2\pi)^3} D(P - k)}, \quad (4)$$

the form of which is established by the Lippman-Schwinger Equation [14] and by demanding that the non-relativistic wavefunction be normalized to unity. Here, $-D(P - k)$ is the propagator denominator of the struck nucleon. We write \mathbf{k}_{rel} to indicate that the argument of the wave function is the **relative** 3-momentum of the two nucleons. Using Eq. (3) with Eq. (4) and using lab frame kinematics yields,

$$F_{m,m'}^0(E_\gamma, l) = 2 \int d^3\mathbf{k} \tilde{\Psi}_{m'}^\dagger(\mathbf{k} - \mathbf{l}/2) \hat{F}(E_\gamma, k, l) \tilde{\Psi}_m(\mathbf{k}) + (n \leftrightarrow p). \quad (5)$$

We stress, at this point, that Eq. (5) does **not** coincide with the conventional VMD-Glauber theory because we have abandoned the usual assumptions that allow us to ignore the \mathbf{k} -dependence in the basic amplitude, which would normally allow us to factor the basic amplitude out of the integral and leave us with the product of the basic amplitude with the non-relativistic form factor. For heavier vector mesons (like the ϕ -meson), the vector meson mass may not be negligible, and the \hat{s} -dependence of the basic amplitude becomes non-trivial at intermediate photon energies.

2.3 The Double Scattering Amplitude

Having obtained the Born term in Eq. (3), we move on to calculate the double scattering term of Fig. 2. Applying the effective Feynman diagrammatic rules, we obtain

$$\begin{aligned} F_{m,m'}^1(s, t) = & \\ & - \int \frac{d^4 p_s}{i(2\pi)^4} \frac{d^4 p'_s}{i(2\pi)^4} \frac{\Gamma_{m'}^\dagger(P + l - p'_s) \bar{F}(\bar{s}, \bar{t}) \hat{F}(\hat{s}, \hat{t}) \Gamma_m(P - p_s)}{[p_s^2 - m_N^2 + i\epsilon] [p'_s^2 - m_N^2 + i\epsilon] [(P - p_s)^2 - m_N^2 + i\epsilon]} \quad (6) \\ & \times \frac{1}{[(P + l - p'_s)^2 - m_N^2 + i\epsilon] [(q - l + p'_s - p_s)^2 - M_V^2 + i\epsilon]} + (p \leftrightarrow n). \end{aligned}$$

Figure 2 and Eq. (6) express the following sequence of events: The incident photon scatters from a nucleon with center of mass energy, $\sqrt{\hat{s}}$, producing an intermediate state with invariant mass, M_V . The intermediate state propagates through the deuteron before scattering from the other nucleon with center of mass energy \bar{s} . (Bars over variables will indicate that they correspond to the secondary scattering.) We neglect fluctuations of the intermediate state for the present purposes.

Now let us integrate over, $p_{s,0}$ and $p'_{s,0}$. The crosses on the spectator nucleon lines in Fig. 2 indicate that we are taking only the poles corresponding to the situation where these two lines are on-shell. Applying the definition in Eq. (4), we recover the formula quoted in [5],

$$\begin{aligned} F_{m,m'}^1(E_\gamma, l) & \\ = & - \int \frac{d^3 \mathbf{p}_s' d^3 \mathbf{p}_s}{(2\pi)^3} \frac{\tilde{\Psi}_{m'}^\dagger(\frac{1}{2} - \mathbf{p}_s') \bar{F}(\bar{s}, \bar{t}) \hat{F}(\hat{s}, \hat{t}) \tilde{\Psi}_m(-\mathbf{p}_s)}{\sqrt{p_{s,0} p'_{s,0}} [(q - l + p'_s - p_s)^2 - M_V^2 + i\epsilon]}. \quad (7) \end{aligned}$$

The $(p \rightarrow n)$ term is implicit in these equations. Finally, we put this equation into a form that makes the next section slightly more manageable by transforming the variables of integration from p'_s and p_s to $p \equiv (p_s + p'_s)/2$ and

$k \equiv p'_s - p_s$, and we make the redefinitions, $k \rightarrow k + l/2$, and $p \rightarrow p + \frac{l}{4}$. The result of these changes is:

$$\begin{aligned} F_{m,m'}^1(E_\gamma, l) \\ = - \int \frac{d^3 \mathbf{p} d^3 \mathbf{k}}{(2\pi)^3} \frac{\tilde{\Psi}_{m'}^\dagger(\mathbf{p} + \frac{\mathbf{k}}{2}) \bar{F}(\bar{s}, \bar{t}) \hat{F}(\hat{s}, \hat{t}) \tilde{\Psi}_m(\mathbf{p} - \frac{\mathbf{k}}{2})}{m_N \left[(q + k - \frac{l}{2})^2 - M_V^2 + i\epsilon \right]} \\ + (p \leftrightarrow n). \end{aligned} \quad (8)$$

In Eq. (8), we have given the amplitude a superscript, 1, to distinguish it from the Born term.

We will summarize this section by cleaning up our notation and by writing out the correct expressions for the kinematic variables in terms of the integration variables, taking into account the variable transformations that were needed to get Eqs. (5) and (8). We explicitly expand each expression to linear order in nucleon momentum in the lab frame. Furthermore, we assume that nucleon 3-momentum and the exchanged 3-momentum are both small and of the same order of magnitude relative to all masses involved. Subscripts a denote Born amplitude quantities while subscripts b denote double scattering quantities. The variables in each expression are established in the particular diagram under consideration. First, we have,

$$\begin{aligned} \hat{s}_a &= ((P - k) + q)^2 \\ &= m_N^2 + 2E_\gamma m_N + 2E_\gamma k_z + \mathcal{O}(\mathbf{k}^2). \end{aligned} \quad (9)$$

Recalling the variable transformations we made in the double scattering term and noting that \mathbf{p} , \mathbf{k} and \mathbf{l} are all of the same order of magnitude, we have,

$$\begin{aligned} \hat{s}_b &= (q + P - p_s)^2 \\ &= m_N^2 + 2E_\gamma m_N + 2E_\gamma \left(p_z - \frac{k_z}{2} \right) + \mathcal{O}(\mathbf{p}^2). \end{aligned} \quad (10)$$

Note that there is only dependence upon k_z and that \mathbf{k} contributions come into play only at higher order in nucleon momentum. For the rescattering amplitude, we get,

$$\begin{aligned} \bar{s}_b &= (k_V + p_s)^2 \\ &= M_V^2 + m_N^2 + 2E_V m_N - 2E_\gamma \left(p_z - \frac{k_z}{2} \right) + \mathcal{O}(\mathbf{p}^2). \end{aligned} \quad (11)$$

This last value is obtained after the pole in k_z is taken, giving the intermediate state an invariant mass of $k_V^2 = M_V^2$. The values of t to be used in each of these cases is,

$$\hat{t}_a = t \quad (12)$$

$$\hat{t}_b = \left(\frac{l}{2} - k \right)^2 = \left(\frac{l_0}{2} \right)^2 + \frac{l_z k_z}{2} - \left(\frac{l_\perp}{2} - k_\perp \right)^2 + \mathcal{O}(\mathbf{k}^2) \quad (13)$$

$$\bar{t}_b = \left(\frac{l}{2} + k \right)^2 = \left(\frac{l_0}{2} \right)^2 - \frac{l_z k_z}{2} - \left(\frac{l_\perp}{2} + k_\perp \right)^2 + \mathcal{O}(\mathbf{k}^2). \quad (14)$$

In the usual VMD-Glauber theory expression for the double scattering term, one keeps only the perpendicular components of \hat{t} and \bar{t} . The terms proportional to k_z are small and since they come with opposite sign, they tend to cancel if the t -dependence of the basic amplitude is nearly exponential. The terms with l_0^2 are proportional to t^2/M_D^2 . Thus, we continue to neglect both of the first two terms in Eqs. (13) and (14). Finally, we stress that $(P - k)^2 = (M_D - m_N)^2 + \mathcal{O}(\mathbf{k}^2)$ so that the struck nucleon may be treated kinematically as being on shell up to terms quadratic in the nucleon momentum.

By using the kinematic expressions of Eqs. 9 through 14 in Eqs. 5 and 8, we may ensure that the factors multiplying the deuteron wavefunction in each of the integrals is correct to linear order in nucleon 3-momentum (or exchanged 3-momentum).

3 Numerical Estimates and the Relationship with VMD-Glauber Theory

3.1 Differential Cross Section

Now that we have calculated the Born and Double scattering amplitudes, let us set up notation that allows us to express the total differential cross section in terms of the basic amplitudes for γN and $V N$ scattering. We do not discuss any physics in this section, but simply formulate our notation to allow for convenient comparisons between our approach and the standard Glauber-VMD approach.

For any exclusive two body reaction involving incoming particles of mass m_1 and m_2 and center of mass energy squared, s , the differential cross section may be represented as follows:

$$\frac{d\sigma^{m,m'}}{dt} = \frac{1}{16\pi\Phi(s, m_1, m_2)} |F_{m,m'}(s, t)|^2, \quad (15)$$

where,

$$\Phi(s, m_1, m_2) \equiv ((s - m_1^2)^2 + m_2^4 - 2sm_2^2 - 2m_1^2m_2^2). \quad (16)$$

In particular, the differential cross section for the reaction in Eq. (1) is,

$$\frac{d\sigma^{m,m'}}{dt} = \frac{1}{16\pi\Phi(s, 0, m_N)} |F_{m,m'}^0(s, t) + F_{m,m'}^1(s, t)|^2. \quad (17)$$

It follows from Eqs. (2) and (8) that the numerical calculations of Eq. (17) will require as input the amplitudes for both the $\gamma N \rightarrow VN$ and the $VN \rightarrow VN$ interactions.

To proceed, we construct a parameterization of the photo-production differential cross section in a form that will provide a smooth transition to the VMD-Glauber regime by writing,

$$\frac{d\hat{\sigma}^{\gamma N \rightarrow VN}}{dt}(\hat{s}, \hat{t}) = \frac{\hat{n}_0^2}{16\pi} \left(\frac{\hat{s}}{\hat{s}_0} \right)^{2(\hat{\alpha}(\hat{t})-1)} \hat{f}^2(\hat{t}) \hat{g}^2(\hat{s}, \hat{t}), \quad (18)$$

for the basic $\gamma N \rightarrow VN$ interaction. In the high energy photon limit, the function $\hat{f}(\hat{t})$ reduces to the usual exponential dependence, $e^{\hat{B}\hat{t}/2}$, with the constant \hat{B} that is typically used to parameterize experimental data as in, for example, Ref. [1]. The Regge trajectory is $\hat{\alpha}(t) = \hat{\alpha}'t + \hat{\alpha}_0$. The factor of $(\frac{s}{s_0})^{\hat{\alpha}(\hat{t})-1}$ is the Regge parameterization obtained in the VMD-Glauber regime and $\hat{g}(\hat{s}, \hat{t})$ is a function which adjusts for other s and t dependence that may appear in the intermediate energy regime, but such that $\hat{g}(\hat{s}, 0)(\frac{s}{s_0})^{\hat{\alpha}(0)-1}$ reduces to 1 in the high energy photon limit. By substituting Eq. (18) into Eq. (15), we obtain,

$$\hat{F}^{\gamma N \rightarrow VN}(\hat{s}, \hat{t}) = \hat{n}_0(\hat{s} - m_N^2) \left(\frac{\hat{s}}{\hat{s}_0} \right)^{\hat{\alpha}(\hat{t})-1} \hat{f}(\hat{t}) \hat{g}(\hat{s}, \hat{t})(i + \hat{\eta}). \quad (19)$$

The overall normalization is labeled \hat{n}_0 and is not necessarily related to a total cross section. The variable, $\hat{\eta}$, is a possible real contribution to the amplitude. Because $P_V \gtrsim 1$ GeV for the kinematic regime under consideration (see Sec. 2.1), the parameterization we use for the $VN \rightarrow VN$ simply takes the diffractive form,

$$\bar{F}^{VN \rightarrow VN}(\bar{s}, t) = \sigma_{VN}(\bar{s})(i + \bar{\eta}) \sqrt{\Phi(\bar{s}, m_N, M_V)} \bar{f}(\bar{s}, \bar{t}). \quad (20)$$

The function, $\bar{f}(\bar{s}, \bar{t})$ reduces to a Regge parameterization, $(\frac{\bar{s}}{\bar{s}_0})^{\bar{\alpha}(\bar{t})-\bar{\alpha}(0)} e^{\bar{B}\bar{t}/2}$ in the VMD regime. By applying the optical theorem to Eq. (20), we see that $\sigma_{VN}(\bar{s})$ is, indeed, the total VN cross section. The variable, $\bar{\eta}$ is a possible real part of the amplitude.

Our peculiar choice of notation is made so that we may smoothly recover the usual Regge parameterizations when we consider the VMD-Glauber approximation. Indeed, applying the VMD hypothesis in the appropriate kinematical regime allows us to assume that $\hat{F}(\hat{s}, \hat{t}) \propto \bar{F}(\bar{s}, \bar{t})$. Thus, applying the optical

theorem allows one to deduce the $VN \rightarrow VN$ amplitude. With the standard high energy approximations, we have,

$$\begin{aligned}\hat{F}(\hat{s}, \hat{t}) &\xrightarrow{E_\gamma \gg M_V} \hat{s}\hat{n}_0(i + \hat{\eta})\hat{s}^{\hat{\alpha}'\hat{t}}e^{\hat{B}\hat{t}/2} \\ \bar{F}(\bar{s}, \bar{t}) &\xrightarrow{E_\gamma \gg M_V} \bar{s}\sigma_{VN}(i + \bar{\eta})\bar{s}^{\bar{\alpha}'\bar{t}}e^{\bar{B}\bar{t}/2}.\end{aligned}\quad (21)$$

Here, we have put $\hat{s}_0 = 1$ GeV for convenience as is often done in parameterizations. In this way, we show how our parameterizations reduce smoothly to the expressions obtained within Regge theory and the VMD hypothesis.

One may fit all of the functions that define the expression for $\hat{F}(\hat{s}, \hat{t})$ directly to data for $\frac{d\sigma^{\gamma N \rightarrow VN}}{dt}$. The function, $\hat{g}(\hat{s}, \hat{t})$ has been introduced to account for peaks in the energy dependence or other irregular energy dependence near the threshold. Without the VMD hypothesis, we can assume no relationship between $\hat{F}(\hat{s}, \hat{t})$ and $\bar{F}(\bar{s}, \bar{t})$. At intermediate energies, therefore, $\bar{F}(\bar{s}, \bar{t})$ must be obtained from a theoretical model or by other experimental means. Conversely, one can use data for the reaction in Eq. (1) to extract $\bar{F}(\bar{s}, \bar{t})$.

3.2 Corrections to Factorizability and an Effective Form Factor

We now define an effective form factor,

$$S_{eff}^{m,m'}\left(E_\gamma, \frac{1}{2}\right) \equiv \int \frac{d^3\mathbf{k}(\hat{s}_a - m_N^2)}{2E_\gamma m_N} \left(\frac{\hat{s}_a}{2E_\gamma m_N}\right)^{\alpha(t)-1} \hat{g}(\hat{s}, \hat{t}) \tilde{\Psi}_{m'}^\dagger\left(\mathbf{k} - \frac{1}{2}\right) \tilde{\Psi}_m(\mathbf{k}), \quad (22)$$

for the Born term, and an effective basic amplitude,

$$\hat{F}_{eff}^0(E_\gamma, t) \equiv 2E_\gamma m_N \hat{n}_0 (i + \hat{\eta}) \left(\frac{2E_\gamma m_N}{s_0}\right)^{\alpha(t)-1} f(t). \quad (23)$$

If we substitute Eq. (19) into Eq. (5), then the Born amplitude for production from the deuteron is,

$$F_{m,m'}^0(E_\gamma, l) = 2\hat{F}_{eff}^0(E_\gamma, l) S_{eff,a}^{m,m'}(E_\gamma, l/2) + (n \leftrightarrow p). \quad (24)$$

The definition in Eq. (23) takes the form of a general diffractive parameterization obtained when one makes the VMD hypothesis. However, Eq. (24) is correct without any approximations. We have recovered the usual structure of the Born expression - the product of a diffractive basic amplitude with a form factor. The new feature in Eq. (24) is that our effective form factor depends on the energy of the photon. The definitions that we made in Eqs. (22) and (23) ensure that the effective form factor and the effective diffractive amplitude

reduce to the usual non-relativistic form factor and the true diffractive basic amplitude in the limit that $E_\gamma \gg M_V$:

$$\begin{aligned} S_{eff}^{m,m'}(E_\gamma, 1/2) &\xrightarrow{E_\gamma \gg M_V} S^{m,m'}(1/2), \\ \hat{F}_{eff}^0(E_\gamma, l) &\xrightarrow{E_\gamma \gg M_V} \hat{F}^{VN \rightarrow VN}(\hat{s}, t). \end{aligned} \quad (25)$$

By following the usual methods of VMD-Glauber theory, one may extract the *effective* amplitude from the $\gamma D \rightarrow VD$ cross section rather than the true amplitude. If, in the region of small $-t$ where the Born cross section dominates, the amplitude for the $\gamma N \rightarrow VN$ scattering is inferred from data using the usual VMD-Glauber theory, then Eq. 24 can be used to obtain a corrected amplitude that accounts for non-factorizability.

3.3 Corrections to Factorizability in Double Scattering

The double scattering term is more complicated due to the fact that, in Eq. (8), the energy dependence cannot easily be factorized out of the integrand. We may rewrite Eq. (8) using Eqs. (19) and (20) as,

$$\begin{aligned} F_{m,m'}^1(E_\gamma, t) = - \int dk_z \int d^2\mathbf{k}_\perp \int \frac{d^3\mathbf{p}}{(2\pi)^3} \frac{\hat{f}(\hat{t}_b) \bar{f}(\bar{s}_b, \bar{t}_b) \tilde{\Psi}_{m'}^\dagger(\mathbf{p} + \frac{\mathbf{k}}{2}) \tilde{\Psi}_m(\mathbf{p} - \frac{\mathbf{k}}{2})}{m_N \left[(q + k - \frac{l}{2})^2 - M_V^2 + i\epsilon \right]} \\ \times \left[\left(\frac{\hat{s}}{s_0} \right)^{\hat{\alpha}(\hat{t})-1} \sqrt{\Phi(\hat{s}, m_N, 0) \Phi(\bar{s}, m_N, M_V)} \right] \\ \times \hat{g}(\hat{s}, \hat{t}) \hat{n}_0 \sigma_{VN}(\bar{s}) (i + \hat{\eta}) (i + \bar{\eta}). \end{aligned} \quad (26)$$

The nonfactorizability of Eq. (26) near threshold comes from the fact that the basic amplitudes and the factors in braces have non-trivial dependence upon the integration variables. We determine that there is no simple reformulation of the integral in Eq. (26) which consistently accounts for corrections linear in momentum. Therefore, we conclude that a direct evaluation is necessary. Note that, though we have set up the integral for a specific parameterization, the analysis applies to any smooth, slowly varying energy dependent basic amplitude. The k_z integral is determined by expanding the denominator in Eq. (26),

$$\begin{aligned} \left(q + k - \frac{l}{2} \right)^2 - M_V^2 + i\epsilon &\approx 2E_\gamma \left[-k_z + \frac{l_z}{2} - \frac{M_V^2}{2E_\gamma} + (k - \frac{l}{2})_0 + i\epsilon \right] \\ &= 2E_\gamma [-k_z - \Delta + i\epsilon]. \end{aligned} \quad (27)$$

The second line fixes the definition of Δ . Notice that by ignoring the term, $(k - \frac{l}{2})^2/2E_\gamma$, we have ignored the possibility of contributions from mesons which are far off shell and which correspond to nucleon 3-momenta that are strongly suppressed by the deuteron wavefunction. Furthermore, note that the pole value of k_z in this approximation only depends on the external variables and is independent of the transverse motion of the nucleons. The resulting double scattering amplitude is then,

$$\begin{aligned}
F_{m,m'}^1(E_\gamma, t) &= \int d^2\mathbf{k}_\perp \int \frac{d^3\mathbf{p}}{(2\pi)^2} \int_{-\infty}^{\infty} \frac{dk_z}{(2\pi)} \frac{\hat{f}(\hat{t}_b) \bar{f}(\bar{s}_b, \bar{t}_b) \tilde{\Psi}_{m'}^\dagger(\mathbf{p} + \frac{\mathbf{k}}{2}) \tilde{\Psi}_m(\mathbf{p} - \frac{\mathbf{k}}{2})}{2E_\gamma m_N [k_z + \Delta - i\epsilon]} \\
&\times \left(\frac{\hat{s}}{s_0} \right)^{\hat{\alpha}(\hat{t})-1} \sqrt{\Phi(\hat{s}, m_N, 0) \Phi(\bar{s}, m_N, M_V)} \hat{g}(\hat{s}, \hat{t}) \hat{n}_0 \sigma_{VN}(\bar{s}_b) (i + \hat{\eta}) (i + \bar{\eta}) \\
&\equiv \int d^2\mathbf{k}_\perp \int \frac{d^3\mathbf{p}}{(2\pi)^2} \int_{-\infty}^{\infty} \frac{dk_z}{(2\pi)} \frac{I_{m,m'}(\mathbf{k}_\perp, k_z, \mathbf{p}, s)}{2E_\gamma m_N [k_z + \Delta - i\epsilon]}.
\end{aligned} \tag{28}$$

We have gathered all factors apart from the energy denominators in the integrand into a function, $I_{m,m'}(\mathbf{k}_\perp, k_z, \mathbf{p}, s)$. Assuming identical protons and neutrons, we get an identical term for the case where the roles of the neutron and proton are inverted. A convenient way to reorganize this formula so that it more closely resembles the non-relativistic quantum mechanical theory is to write the integrand in terms of its Fourier components in the following mixed representation:

$$I_{m,m'}(k_\perp, k_z, \mathbf{p}, s) = \frac{1}{\sqrt{2\pi}} \int_{-\infty}^{\infty} dz \tilde{I}_{m,m'}(\mathbf{k}_\perp, z, \mathbf{p}, E_\gamma) e^{-ik_z z}. \tag{29}$$

The vector meson propagator may be rewritten using the identity,

$$\frac{1}{p - i\epsilon} = \int_{-\infty}^{\infty} dz \Theta(-z) e^{i(p - i\epsilon)z}. \tag{30}$$

Summing the two terms for the neutron and the proton and using the fact that $\Theta(z) + \Theta(-z) = 1$ yields,

$$\begin{aligned}
F_{m,m'}^1(E_\gamma, t) &= i \int \frac{d^3\mathbf{p} d^2\mathbf{k}_\perp}{2E_\gamma m_N (2\pi)^2} I_{m,m'}(\mathbf{k}_\perp, -\Delta, \mathbf{p}, E_\gamma) \\
&- \frac{1}{\sqrt{2\pi}} \int \frac{d^3\mathbf{p} d^2\mathbf{k}_\perp}{2E_\gamma m_N (2\pi)^2} \int_{-\infty}^{\infty} dz \tilde{I}_{m,m'}(\mathbf{k}_\perp, z, \mathbf{p}, s) \sin(-\Delta z) \Theta(z).
\end{aligned} \tag{31}$$

In the VMD-Glauber approximation, $\Delta \rightarrow 0$ and $I_{m,m'}(\mathbf{k}_\perp, 0, \mathbf{p}, s)$ is the usual energy independent density matrix. Hence, the first term in Eq. (31) reduces to the traditional Glauber expression for double scattering and the second term vanishes in the limit where the usual VMD-Glauber assumptions are applicable. The second term is a correction, discussed in Ref. [5] which arises

from the non-zero phase shift in the vector meson wave function induced by longitudinal momentum transfer. In the phase shift term, the factor of $\sin(-\Delta z)$ is itself a correction of order k_z , so we neglect Fermi motion and energy dependent corrections to $I_{m,m'}(\mathbf{k}_\perp, 0, \mathbf{p}, s)$ in the phase shift term.

For a real photon, the double scattering term picks out the relative longitudinal nucleon momentum,

$$\Delta = \frac{l_-}{2} + \frac{M_V^2}{2E_\gamma}. \quad (32)$$

Furthermore, $l_- = -(M_V^2 - t)/2E_\gamma$, so

$$\Delta = \frac{t + M_V^2}{4E_\gamma}, \quad (33)$$

and we see that Δ is indeed negligible at large center of mass energies and small t . Corrections to the double scattering term, at linear order in momentum, arise from performing the integral in the first term of Eq. (31), and by retaining the phase shift term. We end this section by noting that the breakdown in factorization comes simultaneously from the fact that longitudinal momentum transfer is non-negligible, and the fact that the longitudinal momentum of the bound nucleons is non-negligible; the contribution to the basic amplitudes from the longitudinal component of the bound nucleon momentum at linear order would vanish by symmetry in all of the integrals if the longitudinal momentum transfer were neglected in the wavefunctions.

4 Sample Calculations

4.1 Cross Section Calculation

It is usually the case that one calculates the charge and quadrupole form factors in the coordinate space formulation of the form factor. This method reduces the formulae to an extremely simple form and allows one to deal simply and directly with polarizations. For the purpose of modifying the basic amplitude, however, so that it has nucleon momentum dependence, we must maintain the momentum space formulation that results from a direct evaluation of the effective Feynman diagrams in Figs. (1,2). Carrying this procedure out was the topic of the previous two sections. The calculation is straightforward, but becomes numerically cumbersome, and the longitudinal momentum exchanged leads to a breakdown of the orthogonality relations for spherical harmonics that usually lead to a very simple coordinate space formulation. However, dealing with the deuteron polarizations can still be simplified if one chooses the axis of quantization along the direction of momentum ex-

change [15,3]. An overview of the non-relativistic deuteron wave function with polarizations are described in Appendix B.

In this section we provide some sample calculations by using simple models of the basic amplitudes. To this end, we restore the assumption of VMD and we use very simple parameterizations of the s and t dependence in the basic amplitudes. The purpose for doing this is mainly to provide estimates of the sensitivity to non-factorizability rather than because VMD is thought to be appropriate at intermediate energies. We have extracted estimates of the parameters for production of the ρ^0 and ϕ vector mesons from the basic nucleon interaction cross section data appearing in Ref. [1], and we have made rough estimates of the parameterization of the s and t -dependence of these amplitudes (see Sec. A for a description of our parameterizations). This provides us with a reasonable model to work with, though we stress that refinements are ultimately needed. For all of our calculations we use the non-relativistic wavefunction obtained from the Paris N-N potential [16].

We are mainly interested in the ϕ -production cross section which is dominated by natural parity exchange, even at energies close to threshold, due to the OZI rule. However, to demonstrate the consistency of our approach with traditional methods, we consider first the case of the photo-production of ρ^0 -mesons which has been well understood for some time. The basic amplitude for ρ^0 -production is dominated by soft Pomeron exchange at large energies, so that it is constant at high energies, but undergoes a relatively steep rise at energies near threshold due to meson exchanges. The parameterization we use is shown in appendix A. We use a typical exponential slope factor of 7.0 GeV^{-2} for the t -dependence. Fig. (4) shows the cross section for ρ^0 -production at the high energy of $E_\gamma = 12.0 \text{ GeV}$. For comparison, we show data taken at 12.0 GeV from Ref. [1,4]. The comparison with data is reasonable, as it is with the traditional Glauber approach.

Now we consider the more interesting case of ϕ -meson photo-production. At high energy, we use the Regge dependence, $\alpha(t) = .27t + 1.14$ given in Ref.[1]. The parameterization that we used is described further in appendix A. As noted in Ref. [1], the energy dependence of the ϕ -meson photo-production cross section is very weak, but the current state of experimental data is still ambiguous as to how much this energy dependence continues at lower energies. However, the large negative ratio of the real to imaginary part of the amplitude ($\eta = -.48$) [17] suggests that some mechanism other than soft Pomeron exchange is significant. This value of the ratio of the real to imaginary part of the ϕ -meson cross section has large error bars and was calculated neglecting longitudinal momentum transfer. However, it is the only measurement we know of at the moment so we use it for the purpose of demonstration. At lower photon energies, the energy dependence of the basic cross section may become highly non-trivial as is suggested by data in Ref. [18]. The results of the calcu-

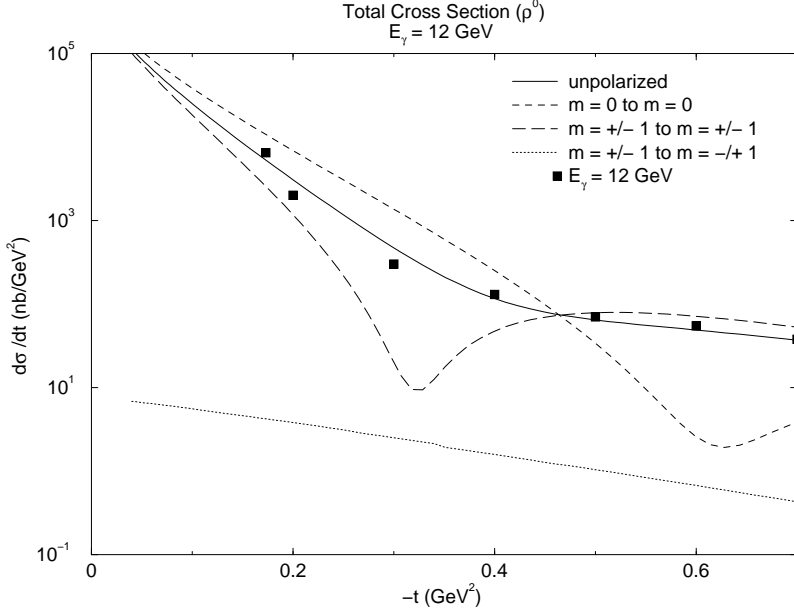


Fig. 4. The unpolarized differential cross section for coherent ρ^0 -meson production compared with the total cross section for different polarizations. The calculation is done with the large photon energy $E_\gamma = 12$ GeV, and the data for $E_\gamma = 12$ GeV is taken from Ref. [1].

lation done with each combination of initial and final deuteron polarizations are shown in the separate panels for a photon energy of $E_\gamma = 30.0$ GeV in Fig. 5 and for a photon energy of $E_\gamma = 3.0$ GeV in Fig. 6. The result is summarized in Figs. 7 and 8 which show the differential cross section for different polarizations along with the unpolarized cross section for photon energies of 30.0 GeV and 3.0 GeV respectively.

Each of the curves in Figs. 5 and 6 separately represents the contribution to the total cross section from a term in the squared amplitude when we apply Eq. 17. The Born and double scattering terms are obtained from the square of Eq. 24 and square of the first term of Eq. 31, respectively. The phase shift term arises from the square of the second term in Eq. 31. We call it the phase shift term because, in the language of non-relativistic quantum mechanical wavefunctions, it arises due to a phase difference between the incoming photon and the produced vector meson. The interference term arises from the interference between Eq. 24 and Eq. 31. Note that the interference term is negative, but it is plotted on the positive axis for demonstration purposes. Note that there is no contribution from the Born term for the $m = +/ - 1$ to $m = -/ + 1$ transition, and therefore the total cross section for the spin-flip reaction has none of the large dips characteristic of the Born cross section.

An important feature that can be seen in Figs. 5 and 6 is that the double scattering term is suppressed in the intermediate energy case relative to the high energy case. We can see this most clearly by comparing the upper left

panel of Fig. 5 with the upper left panel of Fig. 6. It is clear that the double scattering contribution is important in the $E_\gamma = 30$ GeV case at moderate values of $-t$, whereas for the $E_\gamma = 3$ GeV case the cross section is dominated by the Born term all the way up to $-t \approx .4$ GeV². In the general case of multiple scattering from complex nuclei, it is the rescattering contributions which lead to the usual A-dependence (A is the number of nucleons) of Glauber theory. The fact that multiple scattering is suppressed in double scattering in the deuteron suggests that our method would yield a rather different A-dependence from that of usual Glauber theory if it were extended to complex nuclei. Extending our approach to complex nuclei requires further work.

Another problem begins to emerge at lower photon energies and extremely small $-t$ (at $t \approx t_{min}$): A large fraction of the momentum integrals begins to violate relativistic kinematic constraints. It is likely that the basic amplitudes vary extremely rapidly with s and $-t$ in these regions of the integral and that expanding in nucleon momentum is not valid (at least to linear order). In order to make progress, a precise understanding of the dynamics of off-shell amplitudes based on field theory may be necessary. Therefore, our approximation is only valid at $-t$ sufficiently large that the integrand does not contain significant contributions from kinematically forbidden nucleon configurations. We have tested the effect of this region in our calculations, and in performing our calculation, we find that there is virtually no contribution from kinematically forbidden regions for any situation that we consider as long as $-\hat{t} + \hat{t}_{min}$ is greater than a few tens of MeVs. We note that, even at relatively low photon energies, the data is consistent with a smooth exponential $-t$ -dependence (see Ref. [18]) as long as $-t$ is not exactly $-t_{min}$. Note that this theoretical problem of considering t at exactly $-t_{min}$ exists at high energies as well, but that at high energies $-t_{min}$ is generally too small for it to show up in plots. So that we may perform our calculations numerically at all values of $-t$ greater than $-t_{min}$, we choose to make the basic amplitude vanish in kinematically forbidden configurations (when $-t \leq -\hat{t}_{min}$). This results in a small dip just above $-t_{min}$ in our plots. The small dip is, therefore, unphysical, and should be disregarded. We leave it in our plots to illustrate a general failure of the Glauber theory approach at extremely small $-t$ (see Fig. 8 at $-t \lesssim .08$ GeV²); the small dip at extremely small $-t$ denotes a region in which no known multiple scattering formalism works. Numerically, our calculation is only correct in the region of $-t$ higher the dip at small $-t$; that is, when $-\hat{t} + \hat{t}_{min}$ is greater than a few tens of MeVs.

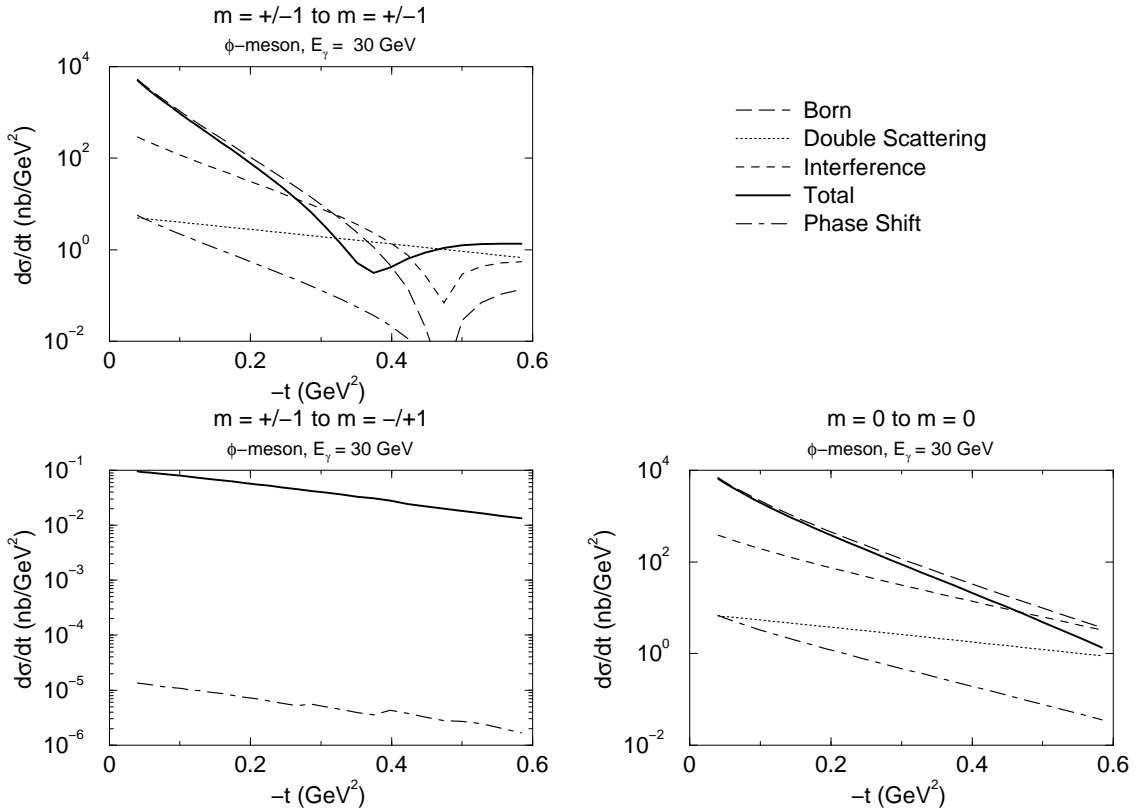


Fig. 5. The long-dashed, dotted, dashed, solid, and dot-dashed lines refer to the Born, double, interference, total, and phase shift terms respectively for a photon energy of $E_\gamma = 30.0$ GeV. For the spin flip cross section, the only non-zero contribution comes from the double scattering term. Note the different scale on the axis for the spin-flip contribution. The interference term is negative but is plotted for illustration on the positive axis.

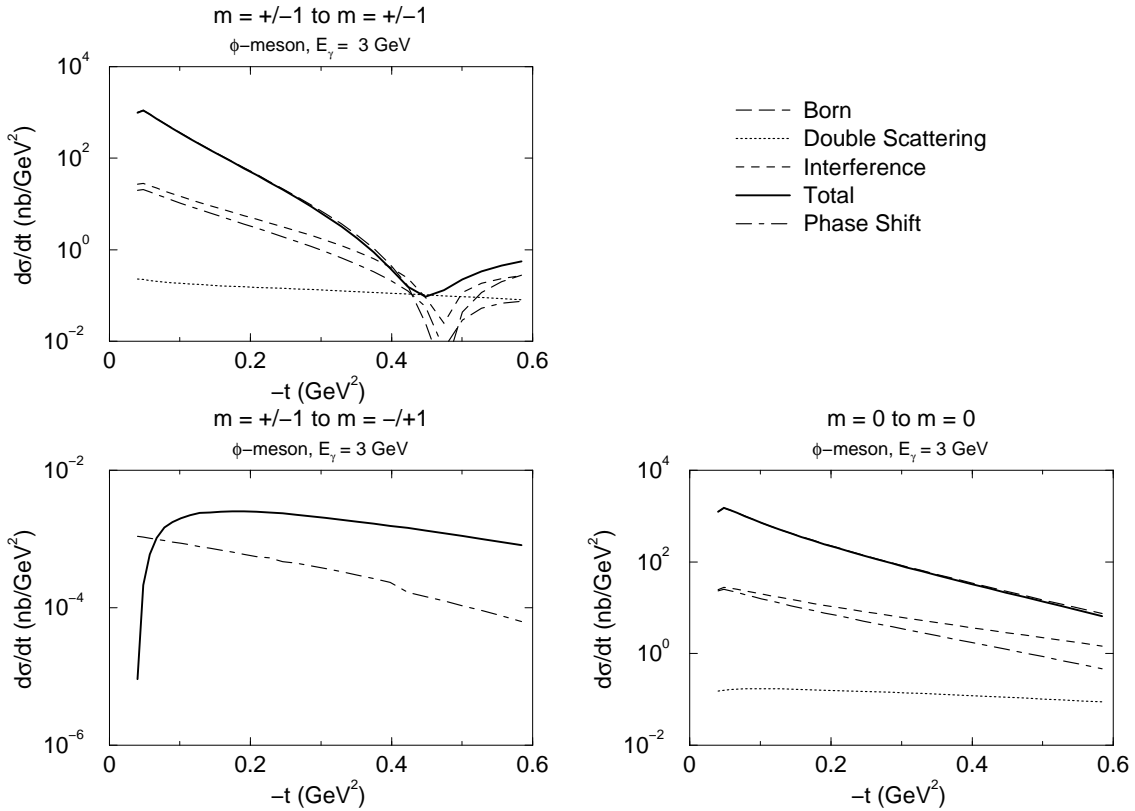


Fig. 6. The long-dashed, dotted, dashed, solid, and dot-dashed lines refer to the Born, double, interference, total, and phase shift terms respectively for a photon energy of, $E_\gamma = 3.0$ GeV. For the spin flip cross section, the only non-zero contribution comes from the double scattering term. Note the different scale on the axis for the spin-flip contribution. The interference term is negative but is plotted for illustration on the positive axis.

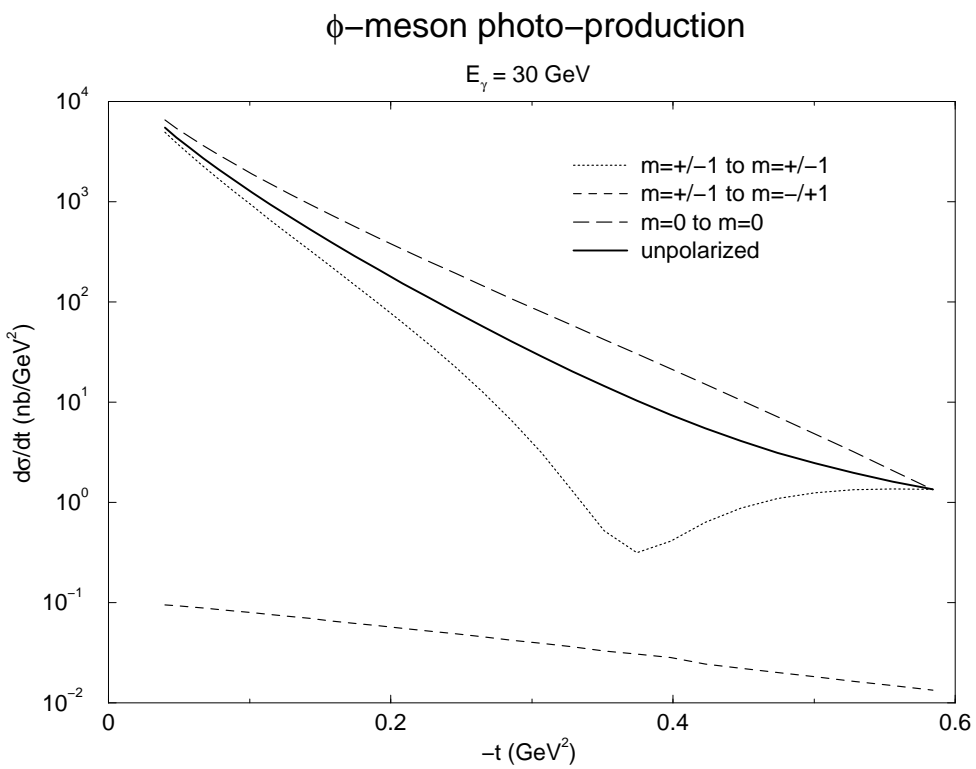


Fig. 7. The differential cross section for ϕ -meson production for different polarizations for a photon energy of $E_\gamma = 30.0 \text{ GeV}$.

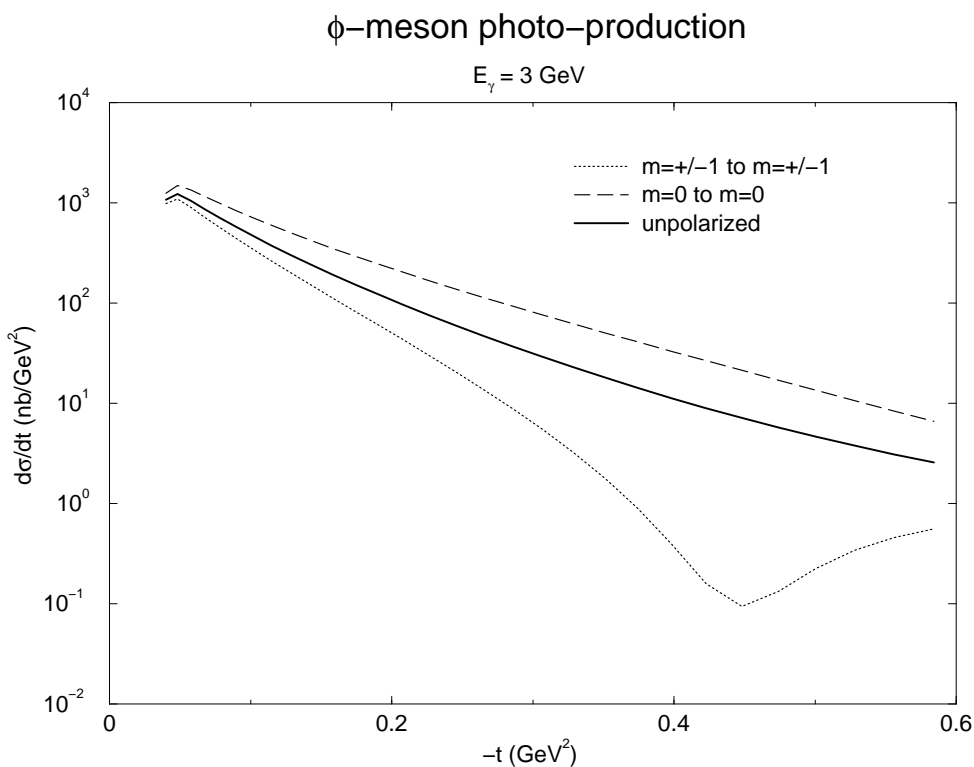


Fig. 8. The differential cross section for ϕ -meson production for different polarizations For a photon energy of $E_\gamma = 3.0 \text{ GeV}$. The deuteron spin flip term is negligible at these energies. The small dip at $-t \lesssim 0.08 \text{ GeV}^2$ is unphysical and should be disregarded.

Next we plot the total unpolarized cross sections as a function of photon energy for a set of fixed values of $-t$. This allows us to compare the factorized and unfactorized calculations directly and to determine approximately at what value of energy the transition to the VMD-glauber regime occurs. Recall that it is the motion of the nucleons in the deuteron (the Fermi motion) that leads to the non-factorizability of the basic amplitudes. Factorization refers the practice of ignoring the dependence of nucleon momentum inside the basic amplitudes when integrals over nucleon momentum are performed. The use of non-factorized amplitudes is the essential difference between our approach and the usual Glauber approach.

First, we have shown the result for ρ^0 -production in Figs. 9 and 10. The solid curves are calculated using our approach whereas the dotted curves are calculated by ignoring nucleon momentum in the basic amplitudes. We remark that the effect of non-factorizability on the ρ^0 -meson cross section is small (less than 10 percent) for the whole range of energies under consideration and for both large and small $-t$. This is consistent with the fact that the usual factorized Glauber approach works well for the light ρ^0 -meson. However, for low energies, the effect of non-factorizability on the ϕ -meson cross section is not negligible as we will now discuss.

We have plotted the energy dependence at fixed t for ϕ -meson production from the deuteron in Figs. 11 and 12. In Fig. 11 we show the energy dependence for $-t = .04 \text{ GeV}^2$. We have only plotted the energy down to $E_\gamma = 5 \text{ GeV}$, because at lower energies, the value of $-t = .04 \text{ GeV}^2$ quickly becomes close to or less than $-t_{min}$. At the higher energies plotted, we observe the near agreement between the two methods of doing the calculation. Even at the lowest energy plotted, the difference between the two methods is less than 10 percent. This plot illustrates that, in the case of extremely small $-t$, we must restrict our consideration to larger energies if we hope to perform reasonable calculations.

In Fig. 12 there is nearly a 30 percent suppression of the factorized cross section relative to the unfactorized cross section at the lowest energy, $E_\gamma = 3 \text{ GeV}$, shown on the plot. Note the rise in the cross section that occurs when we remove the factorization assumption. This effect is mainly due to the suppression of multiple scattering when non-factorizability is taken into account. To see this, note that At $-t = .14 \text{ GeV}^2$ the main effect of double scattering in the usual Glauber approach is to produce a large negative cross term that has a canceling effect. All terms apart from the Born term and the interference term are negligible at this value of t . (See, for example, the upper left panels of Figs. 5 and 6.) Therefore, if multiple scattering is suppressed, as it is in our approach, then the absolute value of the cross term becomes smaller, and the Born contribution is no longer suppressed by multiple scattering. Thus, the curve representing our approach in Fig. 12 is larger than what is

found in the standard Glauber calculation. We emphasize that this result is for a photon energy (3 GeV) that is well into the kinematic region where the eikonal approximation may be applied (see Sec. 2.1), and that $-t = .14 \text{ GeV}^2$ is certainly large enough relative to $-t_{min} = .036 \text{ GeV}^2$ that there are none of the problems discussed earlier related to nearness to $-t_{min}$. Therefore, our method of calculation is ideally suited to the kinematics of Fig. 12, where an effect from the break down of the factorizability assumption is already seen.

At high energies we expect the two methods to agree, and they do within the range of experimental uncertainties of non-relativistic deuteron form factors. The fact that the two methods have slight disagreement at high energies is a reflection of the fact that, even at high energies, we have not calculated the form factor with exactly the same approximation as in the usual Glauber approach. In the usual non-relativistic form factor, any dependence on longitudinal transferred momentum is ignored. If one takes into account exact kinematics, one finds that there are two distinct effects which may cause this assumption to be violated. It is easiest to see this by writing out the exact expression for the transferred longitudinal momentum:

$$l_z = -\frac{t}{2M_D} + \frac{M_V^2 - t}{2E_\gamma}. \quad (34)$$

From this we see that there are two approximations that are normally made in the Glauber approach that allow one to neglect l_z . The first is the ultra-relativistic approximation for the incident vector meson, $E_\gamma \gg M_V$, and the second is the non-relativistic approximation for the exchanged 4-momentum, $-t \ll M_D$. If t is small relative to M_D then there is still a significant contribution to l_z when M_V is non-negligible relative to E_γ . This is the effect that interests us in this paper. It is safe to use the non-relativistic form factor because the transferred energy is,

$$l_0 = -\frac{t}{2M_D}. \quad (35)$$

On the other hand, as long as t is non-zero, there will be a component of l_z that does not die out with energy. This effect represents the error induced by ignoring relativistic recoil. In the future we plan to generalize the formalism to the case of light-cone wave functions so that it may be extended to higher $-t$.

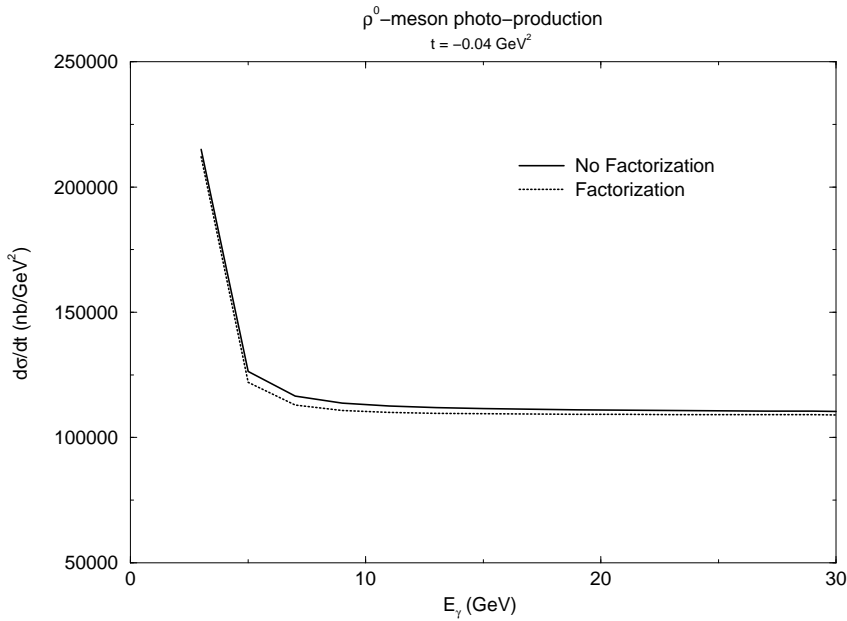


Fig. 9. The energy dependence of the unpolarized differential cross section for ρ^0 -meson photo-production for $t = -0.04 \text{ GeV}^2$. The solid line is the result of our calculation, whereas the dotted line is the result obtained by factorizing the basic amplitude out of the integrals over nucleon momentum.

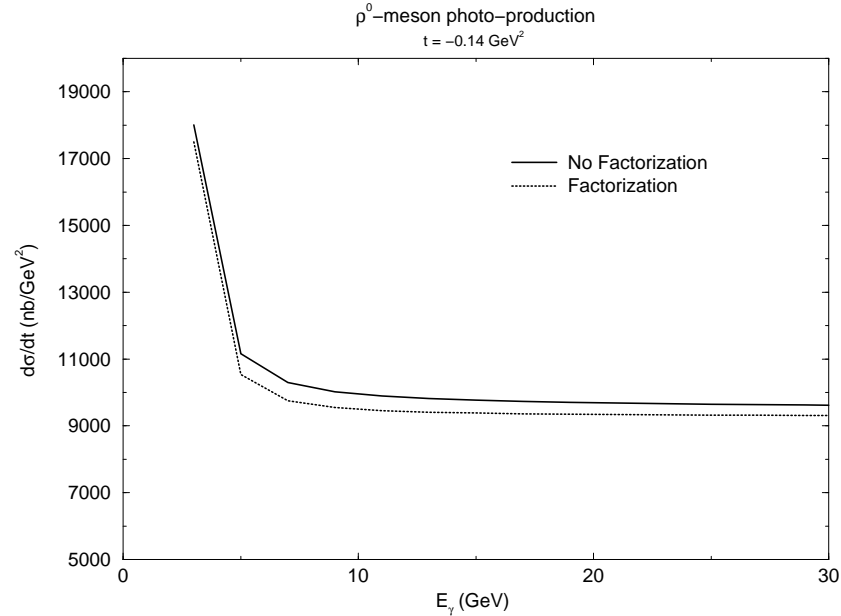


Fig. 10. The energy dependence of the unpolarized differential cross section for ρ^0 -meson photo-production for $t = -0.14 \text{ GeV}^2$. The solid line is the result of our calculation, whereas the dotted line is the result obtained by factorizing the basic amplitude out of the integrals over nucleon momentum.

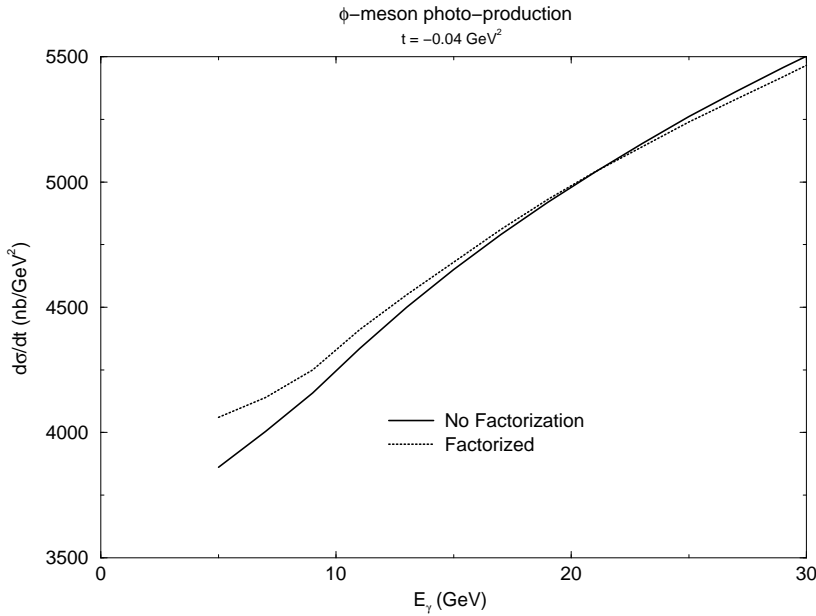


Fig. 11. The energy dependence of the unpolarized differential cross section for ϕ -meson photo-production for $t = -0.04 \text{ GeV}^2$. The solid line is the result of our calculation, whereas the dotted line is the result obtained by factorizing the basic amplitude out of the integrals over nucleon momentum.

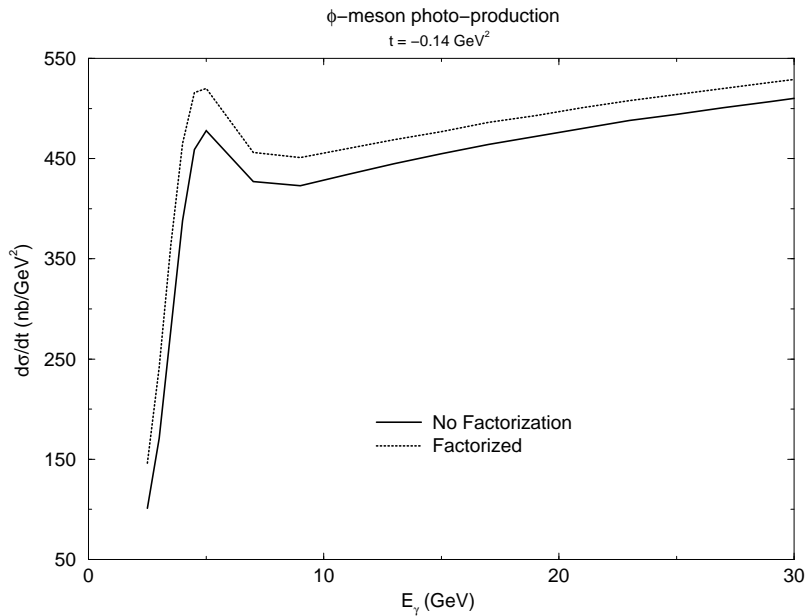


Fig. 12. The energy dependence of the unpolarized differential cross section for ϕ -meson photo-production for $t = -0.14 \text{ GeV}^2$. The solid line is the result of our calculation, whereas the dotted line is the result obtained by factorizing the basic amplitude out of the integrals over nucleon momentum.

5 Directions for Future Work

5.1 Extraction of Basic Amplitudes

Obtaining precise parameterizations of the s and t dependence is one of several steps needed for refinements in the calculation. We note that a peak in the energy dependence has been reported in Ref. [18] for photo-production of ϕ -mesons from a proton target at $E_\gamma = 2$ GeV and it is this data that we used in our parameterization (see Appendix A). We would like to point out, however, that the measurements in Ref. [18] are for the differential cross section at $t = t_{min}$. Therefore, since, the value of t_{min} varies significantly with energy in these near threshold measurements, then the reported measurements give the differential cross section at very different values of t . We have indicated this in Fig. 13(A.). In order to infer the energy dependence at a *fixed* value of t , one needs to assume a form for the t -dependence. The actual t -dependence at these low energies is not well known, but it is straightforward to see that even a simple exponential t -dependence will have an effect on the shape of the overall energy dependence of the cross section. As an example, we have plotted in Fig. 13(A.) the data as it was originally presented in Ref. [18] alongside Fig. 13(B.) where the data have been shifted to a fixed value of t . We have used an exponential slope parameter of 4 GeV 2 which gives reasonable agreement with the data. In the orginal form of the plot, Fig. 13 (A.), the data is shown at a different value of t at each energy. The highest value of $-t_{min}$ occurs at the lowest energy plotted which is around 1.6 GeV. In Fig. 13(B.) we have replotted the energy dependence, but with the value of t for each data point fixed at $-t_{min}$ for $E_\gamma = 1.6$ GeV since this is the largest value of $-t$ that is kinematically allowed for every point on the plot. Let $t_{min}[1.6]$ represent the value of $-t_{min}$ at $E_\gamma = 1.6$ GeV. Then,

$$\frac{d\sigma}{dt} \bigg|_{t=t_{min}[1.6]} = \frac{d\sigma}{dt} \bigg|_{t=t_{min}} e^{4.0 \text{GeV}^{-2}(t_{min}[1.6] - t_{min})}. \quad (36)$$

We use this to obtain Fig. 13 (B.). We see that much of the peak-like behavior is removed. Without a fuller understanding of the t -dependence, therefore, it cannot be ruled out that the observed peak arises from purely kinematical effects. However, the fact that the cross section at fixed t does increase at smaller E_γ is evidence that OZI-violating meson exchange effects become important at these energies.

Recent experimental results also indicate that there may be significant spin effects in the basic amplitudes. Recently preliminary data were reported from SPring-8/LEPS [19] which measured the dependence of the ϕ -meson production at $E_\gamma \sim 2$ GeV on the linear polarization of the photon. Significant polar-

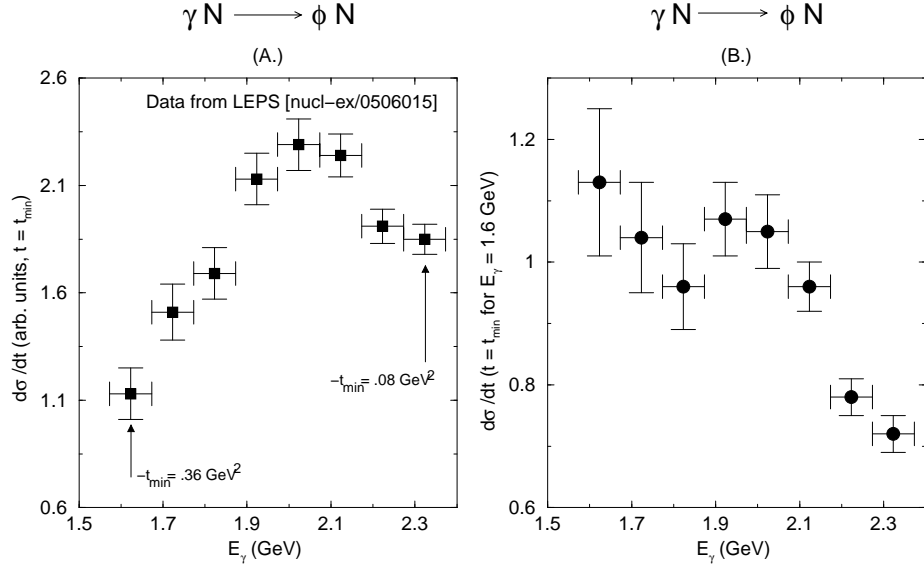


Fig. 13. The is a plot of recent data from LEPS, taken from Ref. [18]. We indicate the significant variation of t_{min} with photon energy. This may have an effect on the over all energy dependence of the cross section. (A.) shows how the data was originally present: at a different value of t for each energy. In (B.) we have shifted all of the data points to the same value of t by assuming a constant slope parameter of 4 GeV^{-2} . Each point in (B.) corresponds to the differential cross section at the fixed value of t corresponding to t_{min} for a 1.6 GeV photon. Note the different scales on the axes in (B.)

ization is observed which requires the presence of a non-vacuum exchange like π, η exchange. Such exchanges lead to spin flip in the nucleon vertex. These contributions for small t are strongly suppressed for coherent production off the deuteron (pion exchange does not contribute in any case due to the zero isospin of the deuteron) they are is determined by the deuteron magnetic form factor which is much smaller than the electric form factor. Hence the coherent production of the ϕ -meson may be used as a spin analyzer of the elementary amplitude in the kinematics where double scattering is a small correction. This topic has already been discussed in Ref. [7]. In the spirit of the original Glauber approach, we have neglected spin effects in this paper for the sake of simplicity. Future work will involve generalizations of our method to the case of spin dependent basic amplitudes.

Before ending our analysis, we mention that, because $V - N$ cross sections are extracted from the multiple scattering term, quantities sensitive to the deuteron polarization would be ideal for testing whether the $V - N$ cross section is unusually large. In order to emphasize this, the cross section for scattering from a polarized deuteron, from $m = +/ - 1$ to $m = +/ - 1$, is plotted in Fig. 14 where the result of using a typical value for the total ϕN cross section (11 mb) is compared with the case when the ϕN cross section is enhanced by a factor of three. (For clarity we have only plotted the sum of all the terms from the squared amplitude rather than each term separately.)

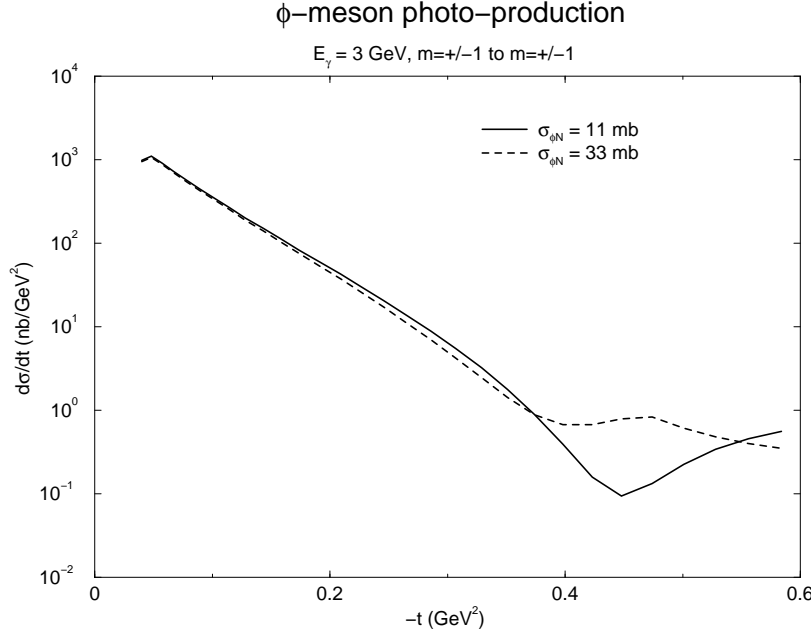


Fig. 14. The energy dependence of the $m = +/ - 1$ to $m = +/ - 1$ differential cross section for ϕ -meson photo-production with $E_\gamma = 3 \text{ GeV}$. The dashed curve shows the result of increasing the typical basic ϕN cross section by a factor of 3.

The sharp dip that normally appears, is due to the sharp dip in the Born cross section. However, the double scattering cross section is nearly flat in $-t$. Therefore, in the summed cross section the double scattering term dominates in the region of the dip, and may even cause the dip to vanish entirely if it becomes very large. Figure 14 shows that, even with the suppression of the double scattering term that results from the non-factorizability that we have been discussing, the dip in the cross section is observed to flatten out when the basic ϕN cross section is abnormally large.

5.2 The Problem of Bound State Amplitudes

We have treated the struck nucleon as being on-shell which is consistent with the neglect of terms quadratic in nucleon momentum. However, immediately at the threshold for particle production, the $\gamma N \rightarrow VN$ amplitude has very unpredictable behavior which may be modified significantly when the nucleon is in a bound state. This is especially clear when we realize that for a given photon energy $-t_{min}$ is different for a deuteron and an on-shell nucleon target. We cannot predict the effects of the off-shellness of the bound nucleon without a complete, relativistic understanding of the basic amplitude. However, we have made predictions in the region of kinematics where it is reasonable to assume that the bound state amplitude is the same as that of the free nucleon amplitude. If one includes dependence upon the nucleon virtuality in the basic amplitude, then one may write the amplitude as $\hat{F}(\hat{s}, \hat{t}, k_N^2)$. For $k_N^2 = m_N^2$, the amplitude reduces to the free nucleon amplitude. As we have stated, $k_N^2 = m_N^2$ up to corrections of order \mathbf{k}_N^2/m_N^2 or higher whereas \hat{s} has linear order corrections in nucleon momentum. Thus, if $\hat{F}(\hat{s}, \hat{t}, k_N^2)$ is an analytic function of kinematic variables, then there will be linear order corrections in nucleon momentum due to \hat{s} whereas the lowest order corrections due to the virtuality of the amplitude are only of quadratic order in nucleon momentum. Of course, all of this depends on the validity of using \mathbf{k}_N/m_N as a small expansion parameter which is only true if the basic amplitude has relatively weak s -dependence. This is one reason why we emphasize that we are consider intermediate energies rather than low energies. One may also include the deuteron binding energy in the calculation of the mass of the bound nucleons, but the binding energy arises from the full consideration of relativistic binding and higher order terms in nucleon momentum, so considering the nucleon binding energy is not consistent with the neglect of higher order nucleon momentum terms or the use of a non-relativistic potential for the N-N interaction.

In this subsection we propose a rough a way to test the validity of the on-shell amplitude approximation. We do this in the next few paragraphs by directly comparing the amplitude when it is evaluated at the value of t_{min} for the deuteron with the case when it is evaluated at t_{min} for a free nucleon with s given by the exact expression for \hat{s} ,

$$\hat{s} = 2E_\gamma \left(M_D - \sqrt{m_N^2 + \mathbf{k}^2} + k_z \right) + \left(M_D - \sqrt{m_N^2 + \mathbf{k}^2} \right)^2 - \mathbf{k}^2. \quad (37)$$

The value of the nucleon 3-momentum thus parameterizes the off-shellness of the bound nucleons. t'_{min} will denote the lower bound of $-t$ for the free nucleon, whereas t_{min} is the lower bound of $-t$ for the deuteron. The struck nucleon inside the deuteron for the unprimed case has \hat{s} given by Eq. (37). We will now consider the case of a free nucleon, with the same \hat{s} as for the

bound nucleon, but with the nucleon on-shell (i.e. $k^2 = m_N^2$) and with a fixed value for k_z . So that the free nucleon energy corresponds to the bound nucleon energy, we will continue to use $M_D - \sqrt{m_N^2 + \mathbf{k}^2}$ for the energy of the struck nucleon. In short, we are comparing t_{min} for γ scattering off a deuteron with t'_{min} for γ scattering off a free nucleon, with energy corresponding to that of the bound nucleon in both cases.

We expect the rate of variation of the basic amplitude with t to be very large near t_{min} . If there is a significant contribution to the integral in Eq. (5) from regions near t_{min} , then t_{min} should nearly equal t'_{min} in order to make the on-shell amplitude a valid approximation to the bound state amplitude. We can use the difference between these two values of t_{min} to estimate the effect of the off-shellness on the amplitude.

In order to test the effect of the off-shellness of the basic amplitude, we may consider two extremes. First, the bound state basic amplitude could be evaluated at the physical value of t for the photon-deuteron process. That is, we could calculate the amplitude, $\hat{F}(\hat{s}, t)$ at t where t is the physical value of t for the photon deuteron process. In this case, since t_{min} is smaller for the deuteron than t'_{min} is for the nucleon, then we are probably over-estimating the cross-section. On the other hand, we could evaluate the basic amplitude at $F(\hat{s}, t - (t_{min} - t'_{min})) = F(\hat{s}, t - \Delta t)$ where t'_{min} is the minimum t for the free, on-shell nucleon. With this second method for choosing which value of t to use in the basic amplitude, the basic amplitude behaves like the free, on-shell nucleon amplitude in the region of t close to t_{min} . Hence, with this method, we are probably underestimating the value of the basic amplitude. In the high energy limit, Δt vanishes and the two amplitudes are equal, and the difference between the two provides an estimate of the off-shell effects. (Note that we must specify a value for \mathbf{k} in order to make a comparison.) Any amplitude which has a relatively slow and smooth variation with t will yield a small difference between $\hat{F}(\hat{s}, t)$ and $F(\hat{s}, t - \Delta t)$. We made this comparison for ϕ -meson production with the parameterization in appendix A and we find only a few percent deviation. We conclude that at a few GeV above threshold it is reasonable to continue using the on-shell amplitude of the nucleon.

6 Summary and Conclusions

The main conclusion of this paper is that the effect of factorization break-down is significant for intermediate photon energies. One may argue, with some justification, that the Glauber approach should be abandoned completely except at very high photon energies. We would point out, however, that the factorization assumption is currently being applied for the ϕ -meson production reaction at energies as low as 1.5 GeV in both experimental and theoretical research.

Therefore, in order to salvage the situation in the energy range of a few GeVs above threshold, we have outlined steps one must follow in order to obtain corrections to leading order in the bound nucleon momentum and transferred momentum. The steps are essentially those of the original Glauber formalism and its extension to vector meson production [3,15,1]; we have started with all of the original assumptions, but we have removed only the assumptions of factorizability, ultra-relativistic kinematics or VMD for the basic amplitudes, and we have formulated everything in the language of covariant diagrams. By using a simple model for the basic amplitude (we restore VMD for the simple model) based on a fit to old and recent data, we have shown that, away from $t = t_{min}$, ignoring Fermi motion (and the resulting breakdown of factorizability) can lead to a significant error in basic cross sections extracted from $\gamma D \rightarrow \phi D$ cross section data (see Fig. 12). This effect will certainly need to be taken into account in future searches for new production mechanisms at intermediate energies. The breakdown in factorizability arrises as a consequence of both the non-negligible longitudinal momentum exchanged, and the non-negligible Fermi motion. An important point is that a key source of the departure from factorizability is the inadequacy of assuming the nearly flat s-dependence predicted by Regge theory in the basic amplitudes. Therefore, models of the basic $\gamma N \rightarrow VN$ amplitude or the $VN \rightarrow VN$ amplitude which depart significantly from nearly flat s-dependence must include *at least* the linear order nucleon momentum corrections of this paper if they are to be used in calculations with a deuteron target. This correction arises purely from the fact that the bound nucleons have non-vanishing momentum and it must be included regardless of the details of a particular model of the basic amplitudes. For the case of ϕ -meson production, we find that our approach is reasonable when we use our particular simple model of the basic amplitude and as long as the photon energy is around 3 GeV or higher and t is not too close to t_{min} .

However, we stress that in a model of the basic $\gamma N \rightarrow VN$ amplitude that predicts much wilder energy dependence at intermediate energies than what we have assumed, the linear order corrections will not be sufficient, and a complete and precise understanding of the $N - N$ interaction and the bound state amplitudes are necessary in order to make a correct calculation. For the ϕ -meson photo-production cross section ($M_\phi \approx 1.02$ GeV), the amplitude may vary wildly with energy at $E_\gamma = 2$ GeV or lower because of the very close proximity to threshold. For both this reason, and the fact that the eikonal approximation begins to break down, we would strongly discourage the extraction of basic amplitudes at photon energies less than or equal to 2 GeV for the ϕ production off the deuteron (or off any nucleus since similar problems will appear for all nuclear targets).

In our sample calculation, we observe that the contribution from double scattering becomes numerically suppressed relative to the Born approximation as

the incident photon energy decreases. However, the multiple scattering terms are what lead to the characteristic A -dependence of the Glauber theory for complex nuclei, $\sigma_{tot} \sim A^{2/3}$. This suggests that an extension of our methods to complex nuclei will yield a rather different A -dependence for the cross section at intermediate energies from what is predicted at high energies. Hence, there will need to be a revision in efforts to extract basic cross sections from nuclear data using extrapolations in A . The extension to complex nuclei, however, requires much more work. We note, however, that data given in Ref. [20] were interpreted as implying a very high ϕN total cross section on the basis of a very traditional Glauber approach at energies of only a few GeVs. Therefore, our next step will be to determine how the non-factorization effects discussed in this paper affect a general, incoherent Glauber series. Furthermore, since it is apparent that spin effects will be important, then a generalization with spin-dependent amplitudes will be needed.

We have purposefully over-simplified our analysis here for the purposes of demonstration. In particular, we have applied the VMD hypothesis at energies where it is suspect and we have neglected fluctuations and $\omega - \phi$ mixing in the intermediate vector meson in the double scattering term. Further analysis will need to include these effects. In order to make further numerical progress, we will need firmer parameterizations of the basic cross sections for vector meson production from nucleons including an overall normalizations. For theoretical work, it would be useful for the purposes of comparison to have a widely agreed upon set of parameterizations.

Finally, we will need a complete understanding of the off-shell amplitudes if we are to take into account the higher order momentum corrections that will be necessary just at the threshold, though we have argued that for smoothly varying basic cross sections, the effect of off-shell amplitudes is small relative to the effect of linear order corrections in nucleon momentum.

Acknowledgements

T.C. Rogers thanks Steve Heppelmann and David Landy for useful discussions, and Isaac Mognet and Nick Conklin for sharing computer facilities. This work is supported by DOE grants under contract DE-FG02-01ER-41172 and DE-FG02-93ER40771.

A Parameterizations

Here we describe the fits of the basic cross sections that we used for our sample calculations. The object here is not necessarily to produce very accurate parameterizations, but rather to devise parameterizations that demonstrate the effects of Glauber factorization while being consistent with recent and established experimental results.

First we consider the $\gamma N \rightarrow \rho^0 N$ differential cross section. For this we use a simple exponential t -dependence with a typical exponential slope of $B = 7.0 \text{ GeV}^{-2}$ and an over all normalization of $105 \mu b/\text{GeV}^2$. (See, e.g. Ref. [1].) It is known that at low energies the normalization undergoes a steep rise. We take this into account in our calculation by including a factor of $(1 + \frac{a}{E_\gamma^4})$ in the overall normalization and then doing a least squares fit to obtain the parameter, a . We find that $a \approx 32.7$. The cross section is thus,

$$\frac{d\sigma}{dt} = 105 \frac{\mu b}{\text{GeV}^2} \left(1 + \frac{32.7 \text{ GeV}}{E_\gamma^4}\right) e^{7.0 \text{ GeV}^{-2} t} \quad (\text{A.1})$$

The result is shown in Fig. A.1. As is seen in the main part of the text, the variation is too weak to introduce a very large effect on the final $\gamma D \rightarrow \rho^0 D$ cross section from Fermi motion.

The case of the ϕ -meson is more complicated due to the irregular behavior near threshold. The main point is to interpolate smoothly between recent low energy and the standard higher energy parameterization. The normalization of the low energy data, taken from recent experimental work in Ref. [18], is obtained from an effective Pomeron and pseudo-scalar exchange model [21] as it was presented in Ref. [18]. We continue to use this so that our model will be consistent with current work. The high energy parameterization was obtained in Ref. [1] by fitting a diffraction-like cross section to a large set of experimental data. We want to interpolate quickly but smoothly between the low energy and high energy data. There is an exponential factor, e^{Bt} , associated with both the high and the low energy behavior, but the slope, B , is around 3.4 GeV^{-2} for the low energy behavior ($E_\gamma \lesssim 4.0 \text{ GeV}$) while it is around 4.8 GeV^{-2} for the high energy behavior. Thus, for the exponential slope we use,

$$B(E_\gamma) = (4.8 - (4.8 - 3.4)e^{-0.001 \text{ GeV}^{-4} E_\gamma^4}) \text{ GeV}^{-2}. \quad (\text{A.2})$$

Next, for the low energy region, there is no Regge slope. That is, $\alpha' = 0$ in the factor, $s^{\alpha' t}$. But, in the high energy region, $\alpha' = .27 \text{ GeV}^{-2}$. Thus, we use,

$$\alpha'(E_\gamma) = .27(1 - e^{-0.001 \text{ GeV}^{-4} E_\gamma^4}) \text{ GeV}^{-2}. \quad (\text{A.3})$$

Now we consider the behavior of $\frac{d\sigma}{dt}|_{\tilde{t}=0}$ for photo-production of the ϕ -meson from a proton target. The high energy parameterization in Ref. [1] is

$$\frac{d\sigma}{dt}\bigg|_{t=0} = 1.34s^{28}, \quad (\text{A.4})$$

and, as in Ref. [1], over-all units will be understood to be $\frac{\mu b}{\text{GeV}^2}$. In order to match to the data of Ref. [18] we want a peak to appear at around $E_\gamma = 2.0 \text{ GeV}$. Therefore, we adjust the parameterization to,

$$\frac{d\sigma}{dt}\bigg|_{\tilde{t}=0} = 1.34s^{28}(1 + ae^{-b(E_\gamma - c)^2}). \quad (\text{A.5})$$

We use Eq.(A.5) to fit to the low energy data of Ref. [18] while assuring that the high energy parameterization of Eq.(A.4) is reproduced at high energies. We find: $a = .71$, $b = 16.5 \text{ GeV}^{-2}$, and $c = 2 \text{ GeV}^{-2}$. Finally, we note that the low energy data is actually given for $t = t_{min}$ rather than $t = 0$. Therefore, we must be sure to include a factor of $e^{B(E_\gamma)t_{min}}$ in the final result for $\frac{d\sigma}{dt}|_{\tilde{t}=0}$. The result of our parameterization for $\frac{d\sigma}{dt}|_{\tilde{t}=0}$ for the ϕ -meson is shown in Fig. A.2. We point out that in the intermediate energy range at around $E_\gamma = 3 \text{ GeV}$, the energy dependence is not completely flat, but it is smooth, and slow enough that its effect may be treated as a small correction.

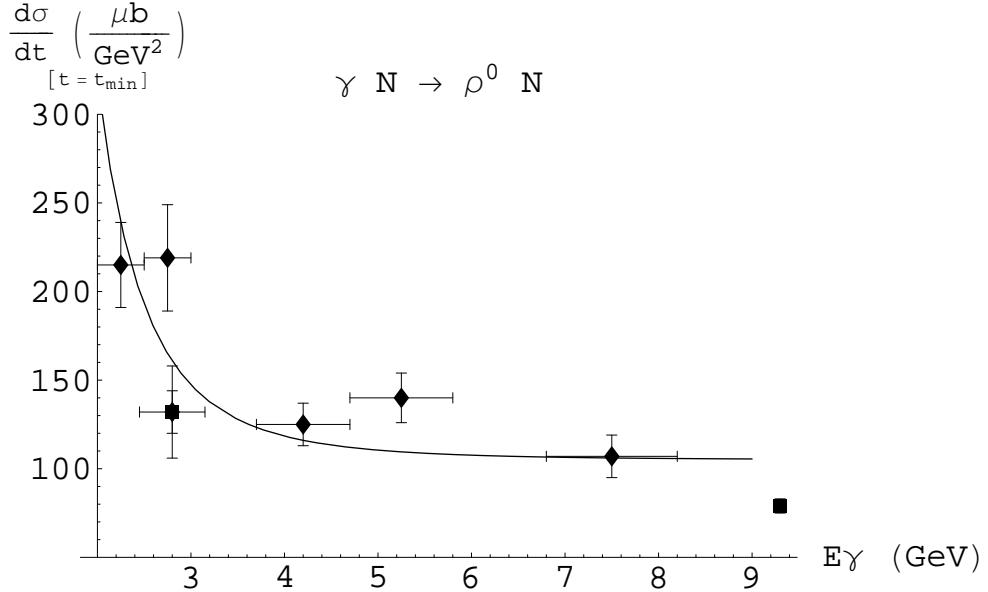


Fig. A.1. We obtain this fit using data from Ref. [22,23,24] (listed in Ref. [1]). We use an inverse-fourth function at low energies and apply a least-squares fit. The peak in the parameterization yields a small effect from Fermi motion (at a few GeVs) because of the small mass of the ρ^0 .

B Deuteron Polarization

In this appendix, we give an over view of the treatment of deuteron spin as it is presented in [15]. In order to evaluate the cross section, we must determine how the operator, $\tilde{\Psi}_{m'}^\dagger(\mathbf{k} - \frac{1}{2})\tilde{\Psi}_m(\mathbf{k})$ acts on the spin-1 ground state of the deuteron. The non-relativistic deuteron wave function in momentum space is written in terms of S and D states via the formula,

$$\tilde{\Psi}_m(\mathbf{k}) = \left[\tilde{u}(k) - 8^{-1/2} \tilde{w}(k) \hat{S}_{12} \right] |\hat{q}, m\rangle \quad (\text{B.1})$$

where,

$$\begin{aligned} \tilde{u}(k) &\equiv \frac{1}{\sqrt{2}\pi} \int_0^\infty r dr j_0(kr) u(r) \\ \tilde{w}(k) &\equiv \frac{1}{\sqrt{2}\pi} \int_0^\infty r dr j_2(kr) w(r). \end{aligned} \quad (\text{B.2})$$

The real functions, $u(r)$ and $w(r)$, are taken from any realistic model of the deuteron wave function, and in our computations we use the Paris potential [16]. The functions, j_0 and j_2 , are the zeroth and second order spherical Bessel functions. In Eq. (B.1), $|\hat{q}, m\rangle$ is a spin-one spinor representing the total angular momentum of the deuteron, and \hat{q} is the quantization axis. The tensor operator, \hat{S}_{12} acts upon the total angular momentum state to produce a sum

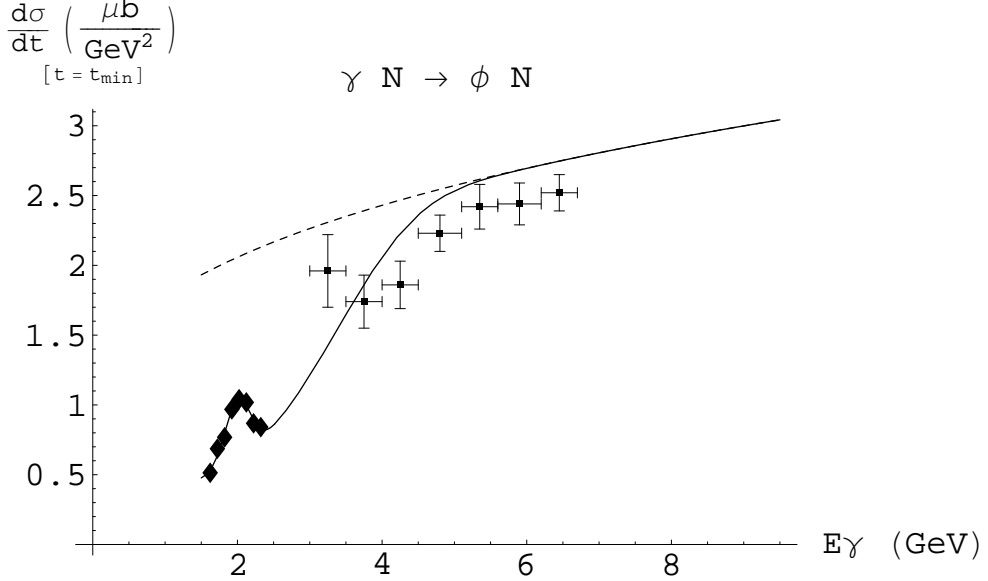


Fig. A.2. The low energy data here is from Ref. [18]. The curve at high energies was taken from Ref. [1]. The dashed curve shows its extension to lower energies. The high energy data is taken from Ref. [25] and is presented to establish the consistency of the high energy parameterization. The curve at low energies has been fit to the low energy data of Ref. [18] using a least-squares fit.

over total spin states. In terms of the spins of the nucleons, it is given by:

$$\tilde{S}_{12} = \frac{3(\sigma_1 \cdot \mathbf{r})(\sigma_2 \cdot \mathbf{r}) - \sigma_1 \cdot \sigma_2}{r^2}. \quad (\text{B.3})$$

The projection onto total spin states is,

$$\begin{aligned} \hat{S}|0, \hat{q}\rangle &= \sqrt{\frac{48\pi}{5}}Y_2^1(\theta, \phi)|-1\rangle - \sqrt{\frac{64\pi}{5}}Y_2^0(\theta, \phi)|0\rangle + \sqrt{\frac{48\pi}{5}}Y_2^{-1}(\theta, \phi)|1\rangle \\ \hat{S}|-1, \hat{q}\rangle &= \sqrt{\frac{16\pi}{5}}Y_2^0(\theta, \phi)|-1\rangle - \sqrt{\frac{48\pi}{5}}Y_2^{-1}(\theta, \phi)|0\rangle + \sqrt{\frac{96\pi}{5}}Y_2^{-2}(\theta, \phi)|1\rangle \\ \hat{S}|1, \hat{q}\rangle &= \sqrt{\frac{96\pi}{5}}Y_2^2(\theta, \phi)|-1\rangle - \sqrt{\frac{48\pi}{5}}Y_2^1(\theta, \phi)|0\rangle + \sqrt{\frac{16\pi}{5}}Y_2^0(\theta, \phi)|1\rangle. \end{aligned}$$

The functions, Y , are the usual spherical harmonic functions. With these equations, we can calculate the effective form factor for each polarization, and then sum and average over final/initial deuteron polarizations.

References

- [1] T. H. Bauer, R. D. Spital, D. R. Yennie and F. M. Pipkin, Rev. Mod. Phys. **50**, 261 (1978) [Erratum-ibid. **51**, 407 (1979)].
- [2] R.P. Feynman “Photon-Hadron Interactions” Addison Wesley Longman, Inc., 1972.
- [3] V. Franco and R. J. Glauber, Phys. Rev. **142**, 1195 (1966).
- [4] R.L. Anderson *et al.*, Phys. Rev. D **4**, 3245 (1971); I.D. Overman, Ph.D. thesis, SLAC-140, UC-34, 1971.
- [5] L. Frankfurt, G. Piller, M. Sargsian and M. Strikman, Eur. Phys. J. A **2**, 301 (1998).
- [6] A. I. Titov, T. S. Lee, H. Toki and O. Streltsova, Phys. Rev. C **60**, 035205 (1999).
- [7] A. I. Titov, M. Fujiwara and T. S. H. Lee, Phys. Rev. C **66**, 022202 (2002) [arXiv:nucl-th/0207079].
- [8] Y. s. Oh, J. Korean Phys. Soc. **43**, S20 (2003) [arXiv:nucl-th/0301011].
- [9] L. L. Frankfurt and M. I. Strikman, Nucl. Phys. B **250**, 143 (1985).
- [10] L. L. Frankfurt, W. R. Greenberg, G. A. Miller, M. M. Sargsian and M. I. Strikman, Z. Phys. A **352**, 97 (1995)
- [11] L. L. Frankfurt, M. M. Sargsian and M. I. Strikman, Phys. Rev. C **56**, 1124 (1997); M.M. Sargsian, Int. J. Mod. Phys. E **10**, 405 (2001).
- [12] D. Binosi and L. Theussl, Comput. Phys. Commun. **161**, 76 (2004) [arXiv:hep-ph/0309015].
- [13] G. D. Alkhazov, S. L. Belostotsky and A. A. Vorobev, Phys. Rept. **42**, 89 (1978).
- [14] G.E. Brown and A.D. Jackson “The Nucleon-Nucleon Interaction” North-Holland Publishing Company, 1976.
- [15] V. Franco and R. J. Glauber, Phys. Rev. Lett. **22**, 370 (1969).
- [16] M. Lacombe, B. Loiseau, J. M. Richard, R. Vinh Mau, J. Cote, P. Pires and R. De Tourreil, Phys. Rev. C **21**, 861 (1980).
- [17] H. Alvensleben *et al.*, Phys. Rev. Lett. **27**, 444 (1971).
- [18] T. Mibe *et al.* [LEPS Collaboration], arXiv:nucl-ex/0506015.
- [19] Talk given by Keito HOREI, “Measurement of photoproduction of ϕ -mesons near threshold by SPring-8/LEPS,” Oct. 27, 2005 at the Particles and Nuclei International Conference in Santa Fe, NM - October 24-28, 2005 To appear in the proceedings of PANIC05; <http://panic05.lanl.gov/>

- [20] T. Ishikawa *et al.*, Phys. Lett. B **608**, 215 (2005).
- [21] A. I. Titov and T. S. H. Lee, Phys. Rev. C **67**, 065205 (2003) [arXiv:nucl-th/0305002].
- [22] J. Ballam *et al.*, Phys. Rev. D **5**, 15 (1972).
- [23] Y. Eisenberg, B. Haber, E. Kogan, E. E. Ronat, A. Shapira and G. Yekutieli, Nucl. Phys. B **42**, 349 (1972).
- [24] J. Ballam *et al.*, Phys. Rev. D **7**, 3150 (1973).
- [25] H. J. Behrend *et al.*, Nucl. Phys. B **144**, 22 (1978).